THE UNIVERSITY OF MICHIGAN

INDUSTRY PROGRAM OF THE COLLEGE OF ENGINEERING

THREE STUDIES IN FLUID MECHANICS

Wei Lai

A dissertation submitted in partial fulfillment
of the requirements for the degree of
Doctor of Philosophy in the
University of Michigan
1961

September, 1961

IP-526

Doctoral Committee:

Professor Chia-shun Yih, Chairman
Assistant Professor Walter R. Debler
Professor Arnold M. Kuethe
Associate Professor Hadley J. Smith
Professor Victor L. Streeter

FOREWORD

Three distinct hydrodynamic problems have been studied. The first problem is one of classical hydrodynamics and is entitled "a solution of two-dimensional irrotational flow with a finite cavity." The method of complex variables is used to obtain the solution. The second problem concerns the "flows of an inviscid fluid past a sphere in a pipe". It has attracted the attention of many authors since the year of 1922. An inverse method initiated by Yih is used to obtain the flow patterns. The last problem is "the stability of a revolving fluid with variable density in the presence of a circular magnetic field". It is a topic of modern fluid dynamics. Chandrasekhar's method is used to solve the eigenvalue problem.

The author wishes to express his appreciation to Professor Chia-shun Yih, chairman of the committee, who, with the intention of acquainting the author with a wide range of fluid-mechanics problems and their methods of solution, suggested the above topics. The work was performed under his direction.

The research was partially supported by the Army Research Office through a contract with The University

of Michigan. The author also received a pre-doctorate fellowship from The University of Michigan, which has enabled him to pursue his graduate study with no financial worries during the tenure of the fellowship. Also, the work would have taken a longer time to finish without the use of the facilities of the computing center of The University of Michigan. To all these sources of support, the author wishes to express his sincere appreciation.

TABLE OF CONTENTS

TABLE OF CONTENTS (Continued)

LIST OF TABLES

LIST OF FIGURES

LIST OF FIGURES (Continued)

Figure Page

PART THREE

PART ONE. A SOLUTION OF TWO-DIMENSIONAL IRROTATIONAL FLOW WITH A FINITE CAVITY

I. INTRODUCTION

It is well known that if there are no cavities, the irrotational flow (with no singularities in the flow region) of an incompressible fluid past a plate, that is parallel to the flow at infinity, is unique and trivial. It is just a parallel uniform flow. If cavities are allowed, however, non-trivial solutions may exist. In this part, one such non-trivial solution is obtained.* A finite cavity is assumed to be attached to one side of the plate and the other side of the plate is assumed to be completely wetted by the flow. The flow is steady and two-dimensional. The solution is obtained in the form of a complex potential $w(z)$, where z is a generic point in the physical plane, and $z = x + iy$. The convention $\frac{dw}{dz} = -u + iv$ is used, u and v being velocity components in the directions of increasing x and y respectively. The boundary of the plate and the attached cavity form part of a streamline, on which we shall suppose, without loss of generality, the stream function to be zero. The dynamic condition on the boundary of the

*After the solution was obtained, the writer was informed by Professor C. S. Yih that Professor E. Zarantonelo of the University of Maryland had solved the problem with a different and more general approach. His paper was published in "Journal de mathematique" the 9th series, 1954, pp. 29-80. However, the details of the present solution have not been given by Professor Zarantonello.

cavity is that the pressure p is constant. This, after using Bernoulli equation and neglecting the effect of gravity, can be expressed by $\left|\frac{dw}{dz}\right| = q_c$, where q_c is the constant speed on the free streamline. The condition at infinity to be satisfied is $\frac{dw}{dz} = -U_\infty$ (constant). Furthermore, there must not be any singularity outside of the plate and the cavity. The flow is characterized by the four variables U_∞, q_c, L (the length of the plate), and Γ, the circulation around any closed path enclosing the cavity. A simple dimensional analysis shows that, if a solution exists at all, there must be a relation between the dimensionless parameters $\frac{\Gamma}{q_c L}$ and $\frac{U_\infty}{q_c}$. This relation is obtained in this part.

The flow contemplated being symmetrical, the physical plane is shown in Figure 1, where CBB'C' is the plate and COC' is the free streamline. B and B' are the two stagnation points. Their locations, for fixed L and U_∞, depend on the circulation Γ. When Γ becomes sufficiently large, B and B' may coincide. This situation is found to occur when the ratio $\frac{U_\infty}{q_c}$ is 1/3. When this ratio becomes smaller than 1/3, the stagnation point moves out of the plate. We shall start with the case where the stagnation points are on the plate. Later, it will be seen that the result is also good for the case where the stagnation point is in the interior of the fluid.

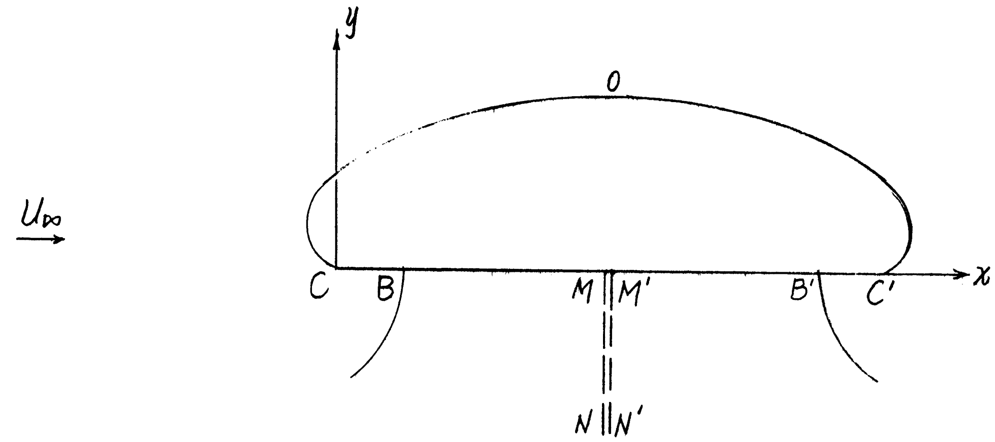

Fig. 1. z-Plane

II. THE w-PLANE AND TRANSFORMATION BETWEEN w AND t

In attempting to solve the problem by the method used in solving the well-known classical free streamline problems, a difficulty is encountered when one attempts a simple mapping from the physical plane to the w-plane. With a circulation involved, the images of the boundaries in the z-plane do not form a closed polygon. This situation can be remedied, however, by inserting two imaginary boundaries MN and M'N', where M and M' are actually the same point, the mid-point of the plate, and MN and M'N' the same line extending to infinity (see Figure 1). From the consideration of symmetry, the potential function ϕ on both MN and M'N' are constants, and if one starts from any point on the line MN and traverses along a path enclosing the cavity until one arrives at any point on the line M'N', the difference in potential function is exactly equal to the circulation Γ. With this in mind, we can transform the physical plane to the w-plane as shown in Figure 2. Note also that for any point on the line MN or M'N', the argument of $\frac{dw}{dz}$ is known. Indeed it is zero. This is important because, if one recalls that in applying the classical method, either the argument or the modulus of $\frac{dw}{dz}$ has to be known along the boundaries for the purpose of constructing Ω-plane ($\Omega = \ln(-q_c\frac{dz}{dw})$), and that they have to be constants in order that images of the boundaries in the Ω-plane can be

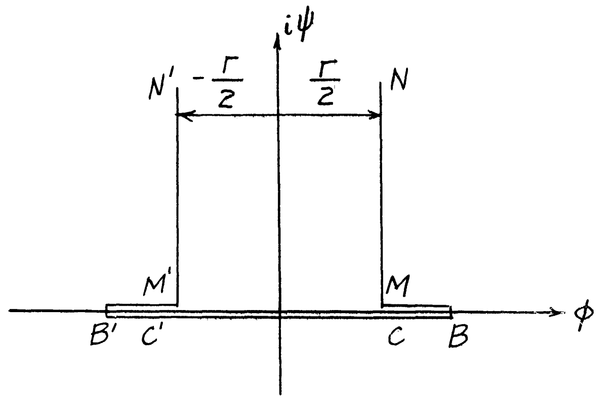

Fig. 2. w-Plane

a polygon so that Schwarz-Christoffel transformation can be used. The w-plane is then mapped into the upper half of an intermediate plane, the t-plane (figure 3).

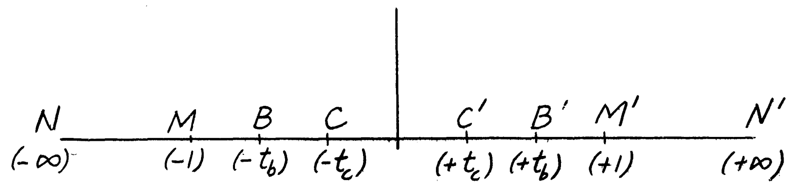

Fig. 3. t-Plane

The Schwarz-Christoffel theorem gives

$$\frac{dw}{dt} = \frac{K_1(t-t_b)(t+t_b)}{\sqrt{(t-1)(t+1)}} = \frac{K_1(t^2-t_b^2)}{\sqrt{t^2-1}} \quad , \qquad (1)$$

where we have chosen arbitrarily to map the points N, M, M' into $-\infty$, -1, $+1$, respectively. Because of symmetry, the point N' goes to $+\infty$ and the points B and B' are located symmetrically at $-t_b$ and $+t_b$.

Integration of equation (1) gives

$$w = K_1\left[\frac{t}{2}\sqrt{t^2-1} + \left(\frac{1}{2}-t_b^2\right)\ln\left(t+\sqrt{t^2-1}\right)\right] + K_2 \ , \tag{2}$$

where

$$K_1 = -\frac{i\Gamma}{\left(\frac{1}{2}-t_b^2\right)\pi} \quad , \qquad K_2 = -\frac{\Gamma}{2} \quad , \tag{3}$$

and

$$\frac{1}{2}-t_b^2<0 \quad , \quad \text{or} \quad t_b > \sqrt{\frac{1}{2}} \ . \tag{4}$$

The relation between t_b and either of the dimensionless parameters $\frac{\Gamma}{q_c L}$ and $\frac{U_\infty}{q_c}$ will be obtained in a later section. We note, however, that when $t_b = 1$, the two stagnation points coincide and when t_b approaches $\sqrt{\frac{1}{2}}$, ϕ_b (the potential at B) approaches infinity.

From equation (2), we obtain that along MBCOC'B'M'

$$\phi = -\frac{\Gamma}{\pi(2t_b^2-1)}\, t\sqrt{1-t^2} + \frac{\Gamma}{\pi}\tan^{-1}\left(\frac{-t}{\sqrt{1-t^2}}\right). \tag{5}$$

III. THE Ω-PLANE AND TRANSFORMATION BETWEEN Ω AND t

With the transformation

$$\Omega = \ln\left(-q\frac{dz}{dw}\right) = \ln\left(\frac{q_c}{q}\right) + i\theta \quad , \tag{6}$$

the physical plane can be transformed into the interior* of a polygon in the Ω-plane (Figure 4), which is then also transformed into the upper half of the t-plane in Figure 3. By doing so, we obtain the relation between $\frac{dz}{dw}$ and w in terms of the parameters t_b and t_c.

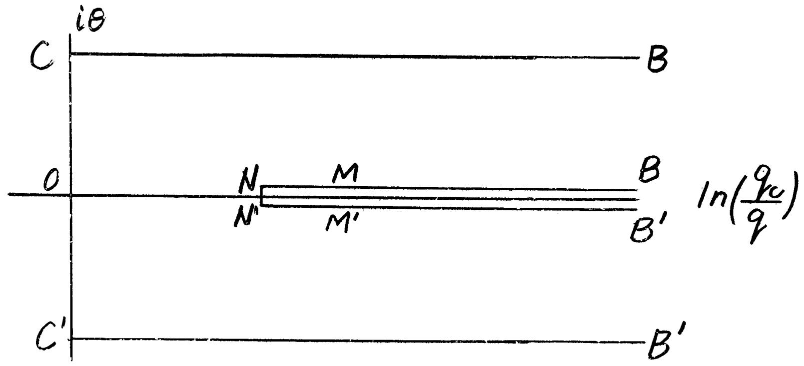

Fig. 4. Ω-Plane

Indeed, the Schwarz-Christoffel method gives

$$\frac{d\Omega}{dt} = \frac{C_1}{(t-t_b)(t+t_b)\sqrt{(t-t_c)(t+t_c)}} \quad , \tag{7}$$

and integration of equation (7) gives

*If one traverses along the boundary in the clockwise direction, the interior region is to the right.

$$\Omega = C_1\left[\frac{1}{-2t_b\sqrt{t_b^2-t_c^2}}\ln\frac{t_b\sqrt{t^2-t_c^2}+t\sqrt{t_b^2-t_c^2}}{t_b\sqrt{t^2-t_c^2}-t\sqrt{t_b^2-t_c^2}}\right]+C_2 \quad , \qquad (8)$$

where $\quad C_1 = -2t_b\sqrt{t_b^2-t_c^2} \quad$ and $\quad C_2 = 0 \quad$. (8a)

Thus

$$-q_c\frac{dz}{dW} = \frac{t_b\sqrt{t^2-t_c^2}+t\sqrt{t_b^2-t_c^2}}{t_b\sqrt{t^2-t_c^2}-t\sqrt{t_b^2-t_c^2}} \quad . \qquad (9)$$

From equation (9), we obtain

$$-q_c\frac{dz}{dW} = \frac{t_b\sqrt{t^2-t_c^2}-t\sqrt{t_b^2-t_c^2}}{t_b\sqrt{t^2-t_c^2}+t\sqrt{t_b^2-t_c^2}} \qquad (10)$$

along NM and MB,

$$-q_c\frac{dz}{dW} = \frac{t_b\sqrt{t^2-t_c^2}+t\sqrt{t_b^2-t_c^2}}{t_b\sqrt{t^2-t_c^2}-t\sqrt{t_b^2-t_c^2}} \qquad (10a)$$

along N'M' and M'B',

$$-q_c\frac{dz}{dW} = \frac{(t_b\sqrt{t^2-t_c^2}-t\sqrt{t_b^2-t_c^2})e^{i\pi}}{-(t_b\sqrt{t^2-t_c^2}+t\sqrt{t_b^2-t_c^2})} \qquad (11)$$

along BC,

$$-q_c\frac{dz}{dW} = \frac{t_b\sqrt{t^2-t_c^2}+t\sqrt{t_b^2-t_c^2}}{t_b\sqrt{t^2-t_c^2}-t\sqrt{t_b^2-t_c^2}} \qquad (11a)$$

along B'C', and

$$-q_c\frac{dz}{dW} = Exp.\left[\, i\,2\tan^{-1}\left(\frac{-t\sqrt{t_b^2-t_c^2}}{t_b\sqrt{t_c^2-t^2}}\right)\right] \tag{12}$$

along COC'.

In the above equations, equations (10) to (12), <u>all square roots are to be taken positive</u>.

At point N, $t = -\infty$, $-q_c\frac{dz}{dw} = \frac{q_c}{U_\infty}$, therefore from equation (10), we get

$$\frac{q_c}{U_\infty} = \frac{t_b+\sqrt{t_b^2-t_c^2}}{t_b-\sqrt{t_b^2-t_c^2}} \quad . \tag{13}$$

IV. GEOMETRY OF THE CAVITY AND THE CLOSURE CONDITION

Along the free streamline COC', $-\frac{\partial\phi}{\partial s} = q_c$. Therefore,

$$\frac{ds}{dt} = -\frac{d\phi}{dt}\frac{1}{q_c} \quad .$$

From equation (5)

$$\frac{d\phi}{dt} = -\frac{2\Gamma}{\pi(2t_b^2-1)}\frac{(t_b^2-t^2)}{\sqrt{1-t^2}} \quad .$$

Therefore

$$ds = \frac{2\Gamma}{q_c\pi(2t_b^2-1)}\frac{t_b^2-t^2}{\sqrt{1-t^2}}\,dt. \tag{14}$$

Now

$$\begin{aligned} dx &= \cos\theta\, ds, \\ dy &= \sin\theta\, ds, \end{aligned} \tag{15}$$

and from equation (12),

$$\theta = 2\tan^{-1}\left(\frac{-t\sqrt{t_b^2-t_c^2}}{t_b\sqrt{t_c^2-t^2}}\right).$$

Therefore

$$\cos\theta = \frac{t_b^2t_c^2-t^2(2t_b^2-t_c^2)}{t_c^2(t_b^2-t^2)} \quad , \tag{16}$$

$$\sin\theta = -\frac{2t_b\sqrt{t_b^2-t_c^2}\;t\sqrt{t_c^2-t^2}}{t_c^2(t_b^2-t^2)} \quad . \tag{17}$$

Thus, along COC',

$$dx = \frac{2\Gamma}{\pi q_c (2t_b^2-1)}\left[\frac{t_b^2}{\sqrt{1-t^2}} - \left(\frac{2t_b^2-t_c^2}{t_c^2}\right)\frac{t^2}{\sqrt{1-t^2}}\right]dt \quad , \tag{18}$$

$$dy = -\frac{4\Gamma}{\pi q_c (2t_b^2-1)} \frac{t_b\sqrt{t_b^2-t_c^2}}{t_c^2} \frac{t\sqrt{t_c^2-t^2}}{\sqrt{1-t^2}} dt . \tag{19}$$

With the origin of the coordinates axis x-y fixed at the left-hand end of the plate (where $t = -t_c$), equations (18) and (19) give, after integration

$$x = \frac{2\Gamma}{\pi q_c (2t_b^2-1)}\left[\left(t_b^2 - \frac{2t_b^2-t_c^2}{2t_c^2}\right)(\sin^{-1}t + \sin^{-1}t_c)\right.$$

$$\left. + \left(\frac{2t_b^2-t_c^2}{2t_c^2}\right)\left(t\sqrt{1-t^2} + t_c\sqrt{1-t_c^2}\right)\right] \quad , \tag{20}$$

$$y = \frac{2\Gamma}{\pi q_c (2t_b^2-1)} \frac{t_b\sqrt{t_b^2-t_c^2}}{t_c^2}\left[\sqrt{1-t^2}\sqrt{t_c^2-t^2}\right.$$

$$\left. + (t_c^2-1)\ln\frac{\sqrt{1-t^2}+\sqrt{t_c^2-t^2}}{\sqrt{1-t_c^2}}\right] \quad . \tag{21}$$

By putting $t = 0$, the half length of the plate is obtained to be

$$\frac{L}{2}=\frac{2\Gamma}{\pi q_c(2t_b^2-1)}\left[\left(t_b^2-\frac{2t_b^2-t_c^2}{2t_c^2}\right)\sin^{-1}t_c+\left(\frac{2t_b^2-t_c^2}{2t_c^2}\right)t_c\sqrt{1-t_c^2}\right] . \tag{22}$$

Along CB and MB,

$$dx=\frac{\frac{d\phi}{dt}}{\frac{\partial\phi}{\partial\chi}}dt.$$

From equation (5),

$$\frac{d\phi}{dt}=-\frac{2\Gamma}{\pi(2t_b^2-1)}\frac{(t_b^2-t^2)}{\sqrt{1-t^2}} .$$

From equation (11),

$$\frac{\partial\chi}{\partial\phi}=\frac{1}{q_c}\left(\frac{-t_b\sqrt{t^2-t_c^2}+t\sqrt{t_b^2-t_c^2}}{t_b\sqrt{t^2-t_c^2}+t\sqrt{t_b^2-t_c^2}}\right) ,$$

or

$$\frac{\partial\chi}{\partial\phi}=\frac{1}{q_c}\frac{(2t_b^2-t_c^2)t^2-t_b^2t_c^2-2t_b\sqrt{t_b^2-t_c^2}\,t\sqrt{t^2-t_c^2}}{t_c^2(t_b^2-t^2)} .$$

Therefore

$$dx=-\frac{2\Gamma}{\pi q_c(2t_b^2-1)}\left[\left(\frac{2t_b^2-t_c^2}{t_c^2}\right)\frac{t^2}{\sqrt{1-t^2}}-\frac{t_b^2}{\sqrt{1-t^2}}\right.$$

$$\left.-\frac{2t_b\sqrt{t_b^2-t_c^2}}{t_c^2}\frac{t\sqrt{t^2-t_c^2}}{\sqrt{1-t^2}}\right]dt . \tag{23}$$

Integration of equation (23) gives

$$x = -\frac{2\Gamma}{\pi q_c(2t_b^2-1)}\Bigg[\left(\frac{2t_b^2-t_c^2}{2t_c^2}\right)\left(-t_c\sqrt{1-t_c^2}-t\sqrt{1-t^2}\right)$$

$$+\left(\frac{2t_b^2-t_c^2}{2t_c^2}-t_b^2\right)\left(\sin^{-1}t+\sin^{-1}t_c\right)+\frac{t_b\sqrt{t_b^2-t_c^2}}{t_c^2}\Bigg\{\sqrt{1-t^2}\sqrt{t^2-t_c^2} \tag{24}$$

$$+(1-t_c^2)\left(\sin^{-1}\frac{\sqrt{1-t^2}}{\sqrt{1-t_c^2}}-\frac{\pi}{2}\right)\Bigg\}\Bigg] \;.$$

The location of the stagnation point B is obtained by putting $t = -t_b$ in equation (24). Thus

$$x_B = -\frac{2\Gamma}{\pi q_c(2t_b^2-1)}\Bigg[\left(\frac{2t_b^2-t_c^2}{2t_c^2}\right)\left(-t_c\sqrt{1-t_c^2}+t_b\sqrt{1-t_b^2}\right)$$

$$+\left(\frac{2t_b^2-t_c^2}{2t_c^2}-t_b^2\right)\left(-\sin^{-1}t_b+\sin^{-1}t_c\right)+\frac{t_b\sqrt{t_b^2-t_c^2}}{t_c^2}\Bigg\{\sqrt{1-t_b^2}\sqrt{t_b^2-t_c^2} \tag{25}$$

$$+(1-t_c^2)\left(\sin^{-1}\frac{\sqrt{1-t_b^2}}{\sqrt{1-t_c^2}}-\frac{\pi}{2}\right)\Bigg\}\Bigg] \;.$$

By putting $t = -1$ in equation (24), we obtain another formula for the half length,

$$\frac{L}{2} = -\frac{2\Gamma}{\pi q_c(2t_b^2-1)}\Bigg[\left(\frac{2t_b^2-t_c^2}{2t_c^2}\right)\left(-t_c\sqrt{1-t_c^2}\right)+\left(\frac{2t_b^2-t_c^2}{2t_c^2}-t_b^2\right)\left(-\frac{\pi}{2}+\sin^{-1}t_c\right)$$

$$+\frac{t_b\sqrt{t_b^2-t_c^2}}{t_c^2}\Bigg\{(1-t_c^2)\left(-\frac{\pi}{2}\right)\Bigg\}\Bigg] \;. \tag{26}$$

Now, in order that there be no gap or overlapping of the flow region, the two equations for half-length of the plate must be identical. This may properly be called the closure condition. If the right hand sides of equation (22) and (26) are equated, the closure condition is obtained, after some algebra,

$$t_c^2 = 1 - \frac{1}{4t_b^2} \quad . \tag{27}$$

Using equation (27), we can eliminate t_c from equations (13) and (22) and obtain

$$\frac{U_\infty}{q_c} = \frac{1}{4t_b^2 - 1} \tag{28}$$

and

$$\frac{\Gamma}{q_c L} = 2\pi \Big/ \frac{4}{(2t_b^2-1)} \left[\frac{2t_b^2-1}{4t_b^2-1} \sin^{-1} \frac{\sqrt{4t_b^2-1}}{2\,t_b} \right.$$

$$\left. + \frac{(8t_b^4 - 4t_b^2 + 1)\sqrt{4t_b^2-1}}{4\,t_b^2(4t_b^2-1)} \right] \quad , \tag{29}$$

in which $\sqrt{\frac{1}{2}} < t_b \leq 1$. Equations (28) and (29) give the relation between the two dimensionless parameters $\frac{U_\infty}{q_c}$ and $\frac{\Gamma}{q_c L}$ in terms of the parameter t_b . When $t_b = 1$, the two stagnation points coincide and equation (28) gives

$$\frac{U_\infty}{q_c} = \frac{1}{3}. \qquad (30)$$

When $\frac{U_\infty}{q_c}$ is smaller than 1/3, the stagnation point B moves into the interior of the fluid. The w-plane, Ω-plane and t-plane for this case are shown in Figures 2a, 3a and 4a respectively, where the points N, M and M' of the w-plane and Ω-plane are again mapped into $-\infty$, -1 and +1 in the t-plane. It is a simple matter to see that equations

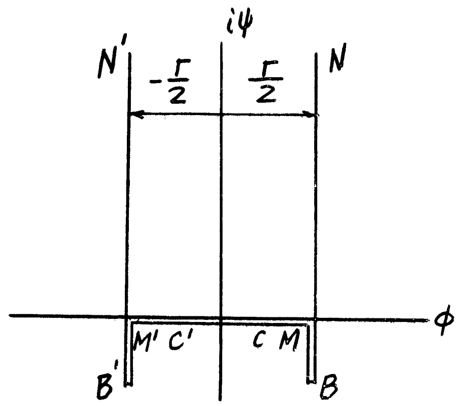

Fig. 2a

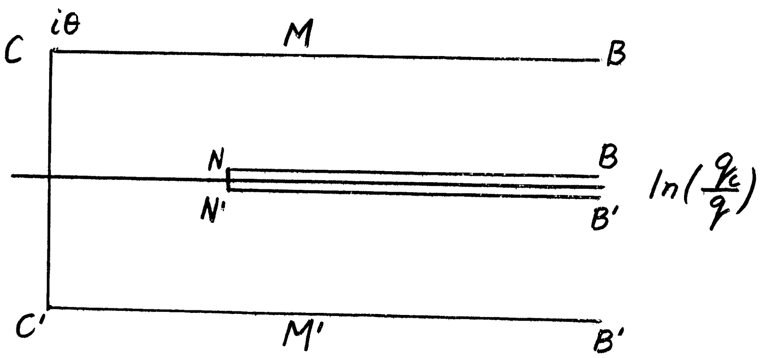

Fig. 3a

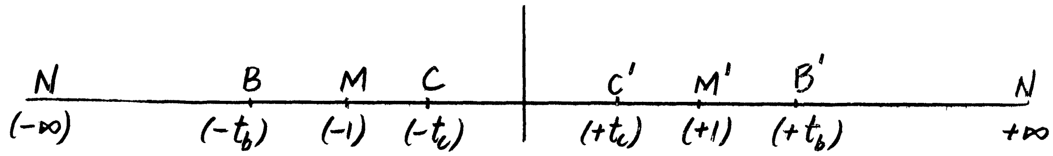

Fig. 4a

(2) and (8) are still the transformation equations and nothing is different except that the range of t_b now has to be larger than unity. This is however automatically insured by equation (28) when $\frac{U_\infty}{q_c}$ is smaller than 1/3.

For the computing of cavity shape, if either $\frac{U_\infty}{q_c}$ or $\frac{\Gamma}{q_c L}$ is given, t_b can be obtained from either equation (28) or equation (29), t_c is then obtained from the closure condition (27) and the cavity shape is then computed from the equations (20) and (21), which can be written in the following dimensionless forms

$$\frac{x}{L} = \left(\frac{\Gamma}{q_c L}\right)\frac{2}{\pi(2t_b^2-1)}\left[\left(t_b^2 - \frac{2t_b^2-t_c^2}{2t_c^2}\right)\left(\sin^{-1}t + \sin^{-1}t_c\right) + \left(\frac{2t_b^2-t_c^2}{2t_c^2}\right)\left(t\sqrt{1-t^2} + t_c\sqrt{1-t_c^2}\right)\right] , \tag{20a}$$

$$\frac{y}{L} = \left(\frac{\Gamma}{q_c L}\right)\frac{2}{\pi(2t_b^2-1)}\frac{t_b\sqrt{t_b^2-t_c^2}}{t_c^2}\left[\sqrt{1-t^2}\sqrt{t_c^2-t^2} + (t_c^2-1)\ln\frac{\sqrt{1-t^2}+\sqrt{t_c^2-t^2}}{\sqrt{1-t_c^2}}\right] . \tag{21a}$$

Two cavity shapes have been computed, they are shown in Figures 5 and 6.

The lift is given by the theorem of Kutta and Joukowski to be

$$L_i = \rho \Gamma U_\infty \quad ,$$

and the lift coefficient is therefore

$$C_L = \frac{L_i}{\frac{1}{2}\rho U_\infty^2 L} = 2\left(\frac{\Gamma}{q_c L}\right)\left(\frac{q_c}{U_\infty}\right) \quad ,$$

in which $\frac{U_\infty}{q_c}$ and $\frac{\Gamma}{q_c L}$ are given by equation (28) and equation (29) respectively.

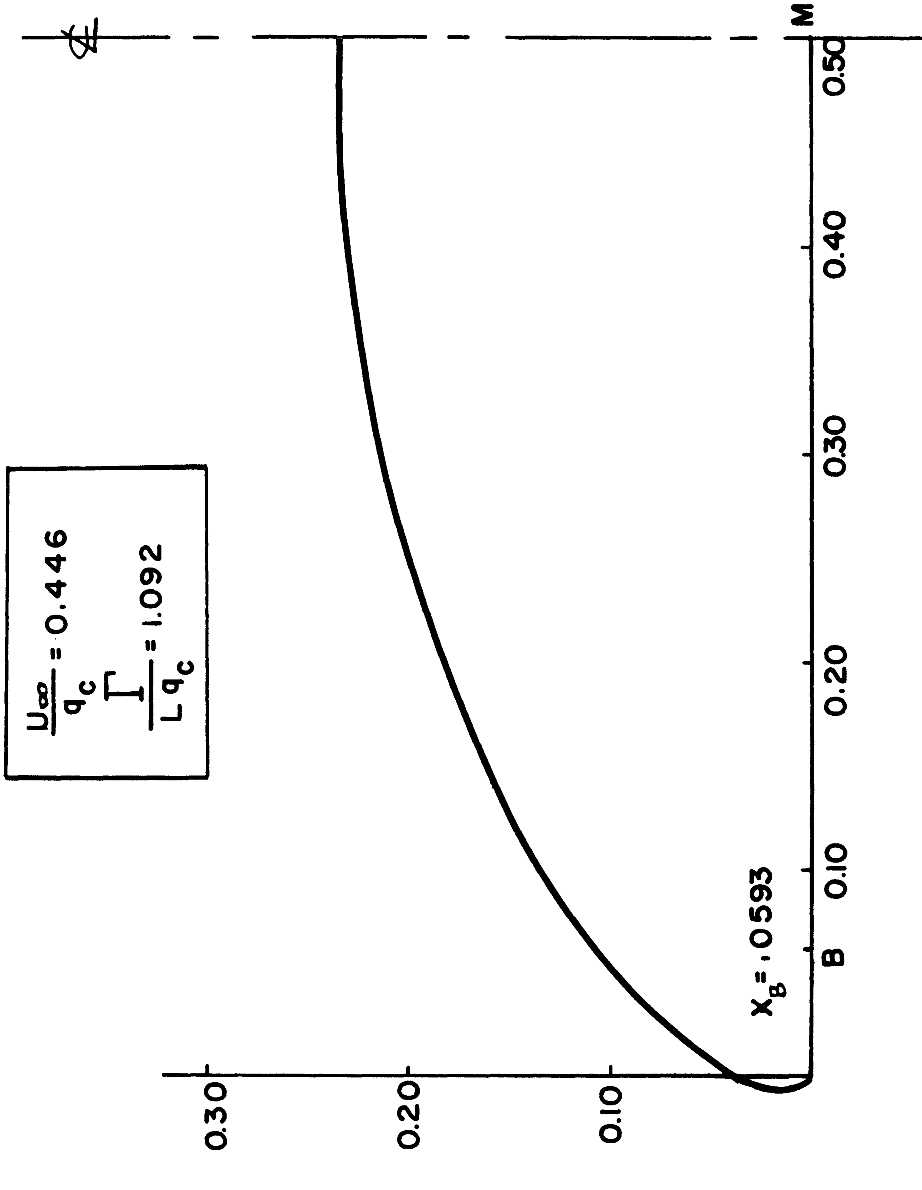

FIG. 5 CAVITY SHAPE FOR $\frac{U_\infty}{q_c} = 0.446$

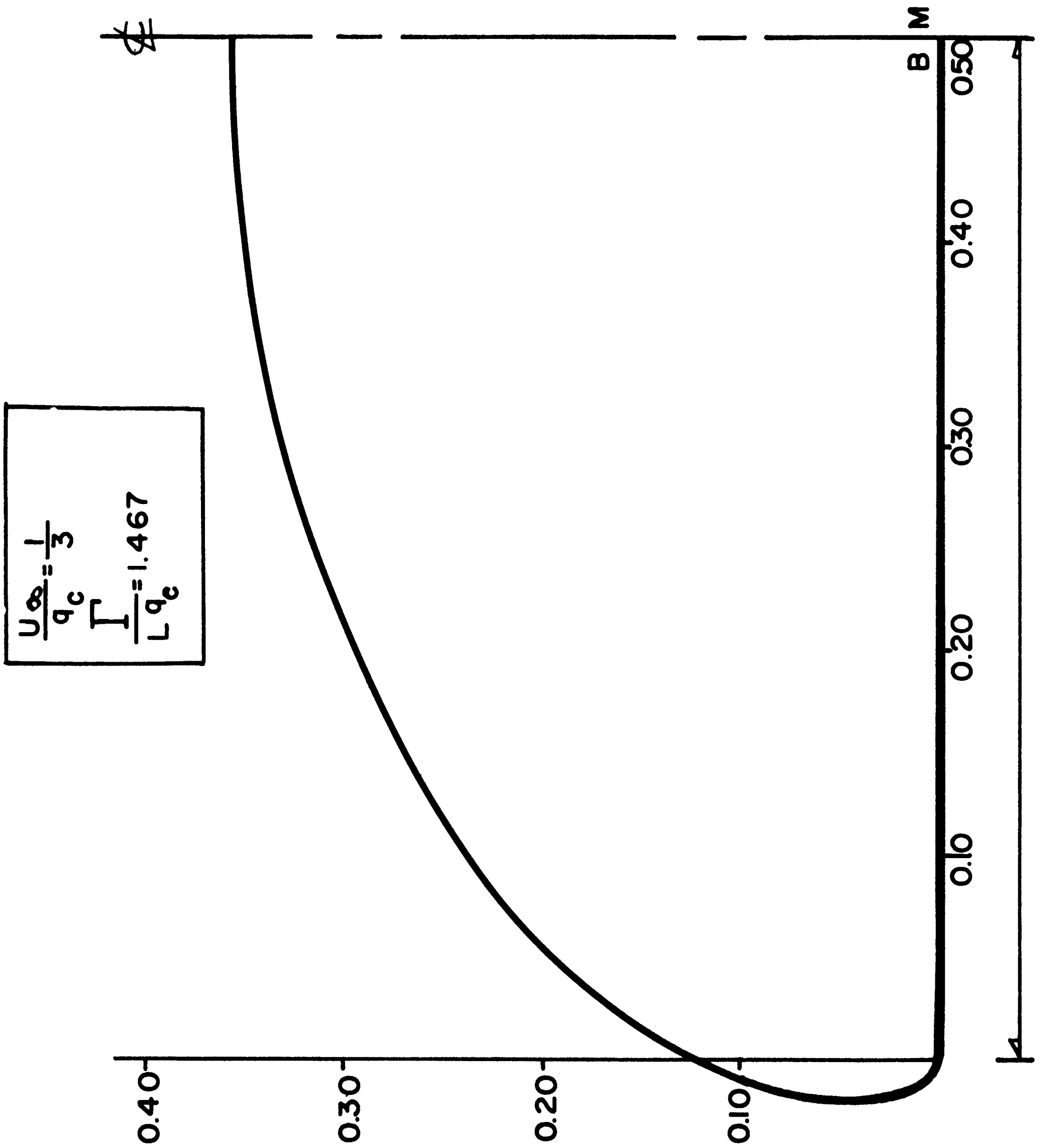

FIG. 6 CAVITY SHAPE FOR $\frac{U_\infty}{q_c} = \frac{1}{3}$

PART TWO. FLOWS OF AN INVISCID FLUID PAST A SPHERE IN A PIPE

I. INTRODUCTION

In this part, an inverse method is used to obtain flow patterns for steady flows of an incompressible, inviscid fluid around a sphere of large size inside a pipe. The center of the sphere is located at the axis of the pipe. Four different types of flow are considered; (1) irrotational flow with constant velocity far upstream, (2) swirling flow with constant axial and angular velocities far upstream, without lee waves, (3) swirling flow with constant axial and angular velocities far upstream, with waves in the lee, and (4) vortex flow with a paraboloid velocity distribution far upstream.

The mathematical difficulties of the above problems have long been recognized. Lamb probably was the first to attempt to solve the irrotational flow case. He has, however, only succeeded in obtaining an approximate solution for spheres of small size. His method will be described later when Fraenkel's solutions for swirling flows are discussed. In 1922, G. I. Taylor gave a solution for swirling flow past a sphere in an unbounded fluid. The solution he gave is indeterminate in that only one boundary condition can be used to determine the two constants in his solution.

Later, Long (1953) showed that the function representing Taylor's particular solution is just one of an infinity of functions comprising the general solution. A critical Rossby number is obtained thereby, above which the flow consists only of a local pertubation that dies out rapidly on both sides of the obstacle and in this case, the presence of a boundary at a finite distance removes the indeterminacy which arises for a body in an unbounded fluid. When the Rossby number is smaller than the critical value, the flow around the obstacle is wave-like and the solution is not unique in the sense that infinitely many upstream conditions are consistent with the solution. However, in this case, uniqueness can be obtained if it is assumed that there are no disturbances far upstream. This assumption is wholly analogous to that made in the classical theory of surface waves (Rayleigh) and is supported by experiment. Even though Long gave the general solution to the governing differential equation, he said "there are great difficulties in finding a solution that satisfies all the conditions in a special case". Fraenkel in 1955 succeeded in obtaining solutions for oval bodies of revolution by using the method of Lamb (1926), and obtained Lamb's solution as a special case where no swirling is present (i.e., irrotational flow). The method Fraenkel used is the following. He first obtained a solution, in terms of Stokes' stream function, for a doublet located on the axis of the singularity). Instead of introducing a doublet at the axis of the pipe, discontinuities of the first derivative, with respect to the direction parallel to the axis of the pipe, of the Stokes' stream function are introduced over a segment of the diameter of the sphere in the plane containing the center of the sphere and normal to the axis of the pipe. This corresponds to introducing a distributed vortex sheet over the segment. The stream function generated from this singularity is indeed very much simpler than that for the doublet obtained by Fraenkel and at the same time one has much more flexibility in choosing the proper singularity function so that obstacles of given smooth boundary (say, spheres) can be obtained with good accuracy. Since the boundary is obtained afterwards, the method is an inverse one. However, when the singularity function is well chosen, the job is really not as hard as one might think. The writer does not claim that a solution for a sphere of any diameter has been obtained. When the diameter is changed, the trial process for the correct boundary has to be performed anew. However, with the help of a computer, this only means the feeding of some other sets of trial data. Furthermore, the results of the present paper do show that the inverse method can be used to obtain useful results which otherwise would be very difficult to get.

II. GOVERNING EQUATIONS

Cylindrical coordinates (r, θ, z) will be used. In these coordinates, the velocity components will be denoted by u, v, and w, respectively. The equations of motion for steady axisymmetric flows are, with viscosity neglected,

$$u\frac{\partial u}{\partial r} + w\frac{\partial u}{\partial z} - \frac{v^2}{r} = -\frac{\partial}{\partial r}\left(\frac{p}{\rho} + \Omega\right) , \tag{1}$$

$$u\frac{\partial v}{\partial r} + w\frac{\partial v}{\partial z} + \frac{uv}{r} = 0 , \tag{2}$$

$$u\frac{\partial w}{\partial r} + w\frac{\partial w}{\partial z} = -\frac{\partial}{\partial z}\left(\frac{p}{\rho} + \Omega\right) , \tag{3}$$

in which z is the axis of symmetry, ρ the (constant) density, and Ω the potential of the external forces (gravity). The equation of continuity for an incompressible fluid is

$$\frac{\partial (ru)}{\partial r} + \frac{\partial (rw)}{\partial z} = 0 . \tag{4}$$

Equation (4) permits the use of Stokes' stream function in terms of which the velocity components can be expressed:

$$u = -\frac{1}{r}\frac{\partial\psi}{\partial z} \quad , \qquad w = \frac{1}{r}\frac{\partial\psi}{\partial r} \quad . \tag{5}$$

Equation (2) expresses the conservation of angular momentum for the same particle, because it can be written as

$$u\frac{\partial(rv)}{\partial r} + w\frac{\partial(rv)}{\partial z} = 0 .$$

Consequently rv is a function of ψ alone. For convenience, we take

$$(rv)^2 = f(\psi) \quad . \tag{6}$$

Furthermore, equations (1) and (3) can be written in the following form:

$$\frac{\partial\chi}{\partial r} = \frac{v^2}{r} + \frac{1}{2}\frac{\partial v^2}{\partial r} - w\eta \quad , \tag{7}$$

$$\frac{\partial\chi}{\partial z} = \frac{1}{2}\frac{\partial v^2}{\partial z} + u\eta \quad , \tag{8}$$

where

$$\chi = \frac{u^2+v^2+w^2}{2} + \frac{p}{\rho} + \Omega \quad , \tag{9}$$

and

$$\eta = \frac{\partial u}{\partial z} - \frac{\partial w}{\partial r} \quad . \tag{10}$$

From equations (7) and (8), together with the continuity equation (4), we have

$$u\frac{\partial \chi}{\partial r} + w\frac{\partial \chi}{\partial z} = 0 \quad . \tag{11}$$

Therefore, χ is also a function of ψ alone. Let

$$\chi = H(\psi) \quad . \tag{12}$$

Using equation (5), and noting that

$$\frac{v^2}{r} + \frac{1}{2}\frac{\partial v^2}{\partial r} = \frac{1}{2r^2}\frac{\partial (r^2v^2)}{\partial r} = \frac{1}{2r^2}\frac{\partial f(\psi)}{\partial r} \quad ,$$

we can write equations (7) and (8) as

$$\frac{\partial H(\psi)}{\partial r} = \frac{1}{2r^2}\frac{\partial f(\psi)}{\partial r} - \frac{1}{r}\frac{\partial \psi}{\partial r}\eta \quad , \tag{13}$$

$$\frac{\partial H(\psi)}{\partial z} = \frac{1}{2r^2}\frac{\partial f(\psi)}{\partial z} - \frac{1}{r}\frac{\partial \psi}{\partial z}\eta \quad . \tag{14}$$

Multiplying (13) by dr, (14) by dz, and adding, we get

$$dH = \frac{1}{2r^2}df - \frac{\eta}{r}d\psi \quad ,$$

or

$$-\frac{\eta}{r} = \frac{dH}{d\psi} - \frac{1}{2r^2}\frac{df}{d\psi} \quad .$$

Since

$$\eta = -\frac{1}{r}\left(\frac{\partial^2\psi}{\partial z^2} + \frac{\partial^2\psi}{\partial r^2} - \frac{1}{r}\frac{\partial\psi}{\partial r}\right) \quad ,$$

we have finally,

$$\frac{\partial^2\psi}{\partial z^2} + \frac{\partial^2\psi}{\partial r^2} - \frac{1}{r}\frac{\partial\psi}{\partial r} = r^2\frac{dH}{d\psi} - \frac{1}{2}\frac{df}{d\psi} \quad . \tag{15}$$

Equation (15) is the governing equation for all the cases mentioned in the introduction. It was originally due to Long (1953). $H(\psi)$ and $f(\psi)$ are to be determined from the conditions far upstream.

CASE (1)

The upstream conditions in this case are characterized by

$w = W$(constant), $u = v = 0$. Thus

$$\psi = \frac{r^2}{2}W \qquad \text{and} \qquad H(\psi) = f(\psi) = 0 \quad .$$

The governing equation is

$$\frac{\partial^2\psi}{\partial z^2} + \frac{\partial^2\psi}{\partial r^2} - \frac{1}{r}\frac{\partial\psi}{\partial r} = 0 \, . \tag{16}$$

CASE (2) and CASE (3)

The upstream conditions are characterized by

$$w = W(\text{constant}),\ u = 0,\ \frac{v}{r} = \omega(\text{constant}).$$

Thus

$$\psi = \frac{r^2}{2}W \quad , \qquad f(\psi) = r^2v^2 = r^4\omega^2 = \Gamma^2\psi^2 \ ,$$

where Γ , the reciprocal of Rossby number, is $\frac{2\omega}{W}$,

$$H(\psi) = \frac{W^2+v^2}{2} + \left(\frac{P_\infty}{\rho} + \Omega\right) = \frac{W^2+v^2}{2} + \frac{v^2}{2} \ ,$$

and

$$\frac{dH}{d\psi} = \frac{d}{d\psi}(v^2) = \frac{d}{d\psi}\left(\frac{2\psi\omega^2}{W}\right) = \frac{1}{2}\Gamma^2 W \ .$$

The governing equation is

$$\frac{\partial^2\psi}{\partial z^2} + \frac{\partial^2\psi}{\partial r^2} - \frac{1}{r}\frac{\partial\psi}{\partial r} + \Gamma^2\psi = \frac{1}{2}r^2\Gamma^2 W \ . \tag{17}$$

CASE (4)

The upstream conditions are $u = v = 0$, and $w = 1 - r^2$.

Therefore

$$\psi = \frac{r^2}{2} - \frac{r^4}{4} \quad , \qquad f(\psi) = 0 \ ,$$

and

$$H(\psi) = \frac{w^2}{2} = \frac{1}{2} - 2\psi \ .$$

The governing equation is

$$\frac{\partial^2\psi}{\partial r^2}+\frac{\partial^2\psi}{\partial z^2}-\frac{1}{r}\frac{\partial\psi}{\partial r}=-2r^2\,. \tag{18}$$

The boundary conditions are the same for all the above equations. They are

$$\psi=0 \quad \text{at} \quad r=0,\ r=1,\ \text{and}\ r^2+z^2=R^2.$$

III. METHOD OF SOLUTION

With a view to satisfying the boundary conditions at r = 0 and r = 1, we can write the solutions for the equations (16), (17) and (18) all in the same form:

$$\psi_- = \psi_0 + \sum_{n=1}^{\infty} A_n e^{+k_n z} r J_1(\lambda_n r) \quad \text{for } z<0 , \tag{19}$$

$$\psi_+ = \psi_0 + \sum_{n=1}^{\infty} B_n e^{-k_n z} r J_1(\lambda_n r) \quad \text{for } z>0 . \tag{20}$$

In equations (19) and (20), J_1 is the Bessel function of the first order and first kind and λ_n are the roots of $J_1(\lambda) = 0$. Thus

$$\lambda_1 = 3.832 , \qquad \lambda_2 = 7.016 , \quad \lambda_3 = 10.173 \quad \text{etc.}$$

For case (1)

$$\psi_0 = \frac{r^2}{2} W , \quad \text{and} \quad k_n = \lambda_n \quad ,$$

for case (2)

$$\psi_0 = \frac{r^2}{2} W , \quad \text{and} \quad k_n = \sqrt{\lambda_n^2 - \sigma^2} , \quad \sigma < \lambda_1 \quad ,$$

for case (3)

$$\psi_0 = \frac{r^2}{2}W\ , \quad and \quad k_n = \sqrt{\lambda_n^2 - \sigma^2}\ , \quad \lambda_N < \sigma < \lambda_{N+1}\ ,$$

and for case (4)

$$\psi_0 = \frac{r^2}{2} - \frac{r^4}{4}\ , \quad and \quad k_n = \lambda_n\ .$$

In cases (1), (2) and (4), k_n are positive and real, therefore, there are no waves. The coefficient A_n and B_n are determined by demanding

$$\psi_- = \psi_+ \quad at \quad z = 0\ , \tag{21}$$

$$\frac{\partial \psi_-}{\partial z} - \frac{\partial \psi_+}{\partial z} = f(r) \quad at \quad z = 0\ , \tag{22}$$

in which $f(r) = 0$ for $r \geqq S < R$, and is chosen such that $\psi = 0$ at $z^2 + r^2 = R^2$.

Since ψ_- and ψ_+ satisfy the governing equation, (21) and (22) ensure that ψ_+ is the analytic continuation of ψ_-, there are no singularities in the domain outside of the sphere.

Now equation (21) demands that

$$A_n = B_n \tag{23}$$

and equation (22) demands that

$$\sum_{n=1}^{\infty} 2k_n A_n r J_1(\lambda_n r) = f(r)\ .$$

Thus

$$A_n = \frac{\int_0^1 f(r)J_1(\lambda_n r)dr}{k_n[J_2(\lambda_n)]^2} \quad . \tag{24}$$

In case (3), k_1, k_2, ...k_n are imaginary, therefore, there are N wave components in the solution. If we demand that there be no waves upstream, then

$$\psi_- = \frac{1}{2}Wr^2 + \sum_{N+1}^{\infty} A_n e^{+k_n z} r J_1(\lambda_n r) \quad \text{for } z<0 , \tag{25}$$

$$\psi_+ = \frac{1}{2}Wr^2 + \sum_{n=1}^{N}(B_n \cos a_n z + C_n \sin a_n z) r J_1(\lambda_n r)$$
$$+ \sum_{N+1}^{\infty} D_n e^{-k_n z} r J_1(\lambda_n r) \quad \text{for } z>0 , \tag{26}$$

where

$$a_n = \sqrt{\sigma^2 - \lambda_n^2} \quad .$$

Now (21) demands that

$$A_n = D_n \quad (n > N), \tag{27}$$

$$B_n = 0 \quad (n \leqq N), \tag{28}$$

and (22) demands that

$$A_n = \frac{1}{k_n[J_2(\lambda_n)]^2}\int_0^1 f(r)J_1(\lambda_n r)dr, \quad (n>N), \tag{29}$$

$$C_n = -\frac{2}{a_n[J_2(\lambda_n)]^2}\int_0^1 f(r)J_1(\lambda_n r)dr, \quad (n \leqq N) \tag{30}$$

C_n's are the amplitudes of the N wave components and the corresponding wave lengths are $\frac{2\pi}{a_n}$. Since there are infinitely many functions f(r) which will give the same C_n's from equation (30), and since different f(r)'s generate different shapes of the obstacle, for the same Rossby number the amplitudes and wave lengths of the lee waves do not depend on the detailed shape of the obstacle but on certain integrals of the singularity function generating the obstacle. Near the obstacle, however, the flow depends on all the Fourier coefficients of f(r), and is therefore greatly effected by the shape of the obstacle.

IV. THE GENERATING FUNCTION f(r)

One generating function has been chosen for the purpose of generating a sphere at the axis of the pipe for all the four cases mentioned in the previous paragraphs. It is

$$\begin{aligned} f(r) &= M(G_1 r^4 + G_2 r^2 + G_3) && \text{for } 0 \leqq r \leqq S \\ &= 0 && \text{for } \quad r \geqq S \ . \end{aligned} \tag{31}$$

The constants G_1, G_2, G_3 and M are of course different not only for each case but also for each different diameter of the sphere. This choice of generating function has proven to be very successful. Among the six flow patterns obtained, two of which have the shape of the obstacle so close to a perfect sphere that the deviations are practically undetectable with reference to the scale of the accompanying drawings. Two others have maximum deviations of less than one percent at the worst points, the other two have maximum deviations of less than two and half percent.

With the generating function given by (31), the coefficients A_n's and C_n's in the above equation are given by

$$A_n = \frac{M}{k_n [J_2(\lambda_n)]^2} \left[G_1 D_1(n) + G_2 D_2(n) + G_3 D_3(n) \right] , \tag{32}$$

$$C_n = -\frac{2M}{a_n [J_2(\lambda_n)]^2} \left\{ G_1 D_1(n) + G_2 D_2(n) + G_3 D_3(n) \right\} , \tag{33}$$

where

$$D_1(n) = \frac{2S^4 J_2(\lambda_n S)}{\lambda_n} - \frac{8S^3 J_3(\lambda_n S)}{\lambda_n^2} + \frac{S^4 J_4(\lambda_n S)}{\lambda_n} \ ,$$

$$D_2(n) = \frac{S^2 J_2(\lambda_n S)}{\lambda_n} \ ,$$

$$D_3(n) = -\frac{J_0(\lambda_n S)}{\lambda_n} + \frac{1}{\lambda_n}$$

V. NUMERICAL RESULTS

For simplicity, W is taken to be unity for cases (1), (2) and (3). For case (4) $W = 1 - r^2$, therefore, maximum velocity is also equal to unity. This amounts to making all the velocity dimensionless through division by Wmax.

Figure 1 is for irrotational flow. The ratio of the diameter of the sphere to that of the pipe is 0.4, the generating function is

$$f(r) = 24.78(3383r^4 + 2r^2 - 1.0) \quad \text{for } 0 \leqq r \leqq 0.13,$$

$$f(r) = 0 \quad \text{for } r \geqq 0.13.$$

Figure 2 is also for irrotational flow. The ratio of the diameters is 0.5, and

$$f(r) = 33.90(700.4r^4 + 2r^2 - 0.8) \quad \text{for } 0 \leqq r \leqq 0.18,$$

$$f(r) = 0 \quad \text{for } r \geqq 0.18$$

Figure 3 is for swirling flow with Rossby number equal 1/3, which is larger than the critical number $1/\lambda_1$. There is no wave in the lee of the sphere. The ratio of the diameters is 0.4, and

$$f(r) = 10.24(1886r^4 + 2r^2 - 1.0) \quad \text{for } 0 \leqq r \leqq 0.15,$$

$$f(r) = 0 \quad \text{for } r \geqq 0.15.$$

Figure 4 is also for swirling flow with Rossby number equal 1/3. The ratio of the diameters is 0.5, and

$$f(r) = 3.697(202.3r^4 + 2r^2 - 1.4) \quad \text{for } 0 \leqq r \leqq 0.28,$$

$$f(r) = 0 \quad \text{for } r \geqq 0.28.$$

Figure 5 is for swirling flow with Rossby number equal 1/4.5, which is smaller than the critical number. There is one lee wave component in the lee of the sphere. The ratio of the diameters is 0.4, and

$$f(r) = 13.46(137.2r^4 + 2r^2 - 1.0) \quad \text{for } 0 \leqq r \leqq 0.28,$$

$$f(r) = 0 \quad \text{for } r \geqq 0.28.$$

Figure 6 is for vortex flow. The velocity distribution far upstream is a paraboloid. The ratio of the diameters is 0.5, and

$$f(r) = 100.3(7800r^4 + 2r^2 - 0.8) \quad \text{for } 0 \leqq r \leqq 0.10,$$

$$f(r) = 0 \quad \text{for } r \geqq 0.10.$$

Even though the flow patterns look very much alike between Figure 1 and Figure 3 and also between Figure 2 and Figure 4, the effect of swirling is nevertheless clearly seen. The streamlines in the neighborhood of the sphere in Figures 3 and 4 are farther away from the sphere than the corresponding streamlines in Figures 1 and 2. Figure 5 shows a very interesting flow pattern. In that figure, the swirling is large enough to have one wave component in the lee of the sphere. There is a succession of big eddies, with sizes that are bigger than that of the sphere, in the lee of the sphere. It should be noted that since the flow in the eddies does not originate at infinity, there is no a priori reason why equation (17) should govern the flow in the eddies. The details of the eddy flow may be significantly different from that given in the figure.

The flow pattern in the upstream side of the sphere in Figure 6 probably represents the flow of a real fluid (when the upstream flow is laminar) past a stationary sphere better than Figure 1 does, because the upstream condition is more realistic in Figure 6. However, when the sphere is moving along the axis with an uniform velocity and the fluid at infinity is either at rest or rotating as a rigid body, Figures 1 to 5 are more realistic.

VI. CONCLUSION

From the results of the present part, an inverse method has been shown to be very useful in constructing certain flow patterns that are otherwise very difficult to do.

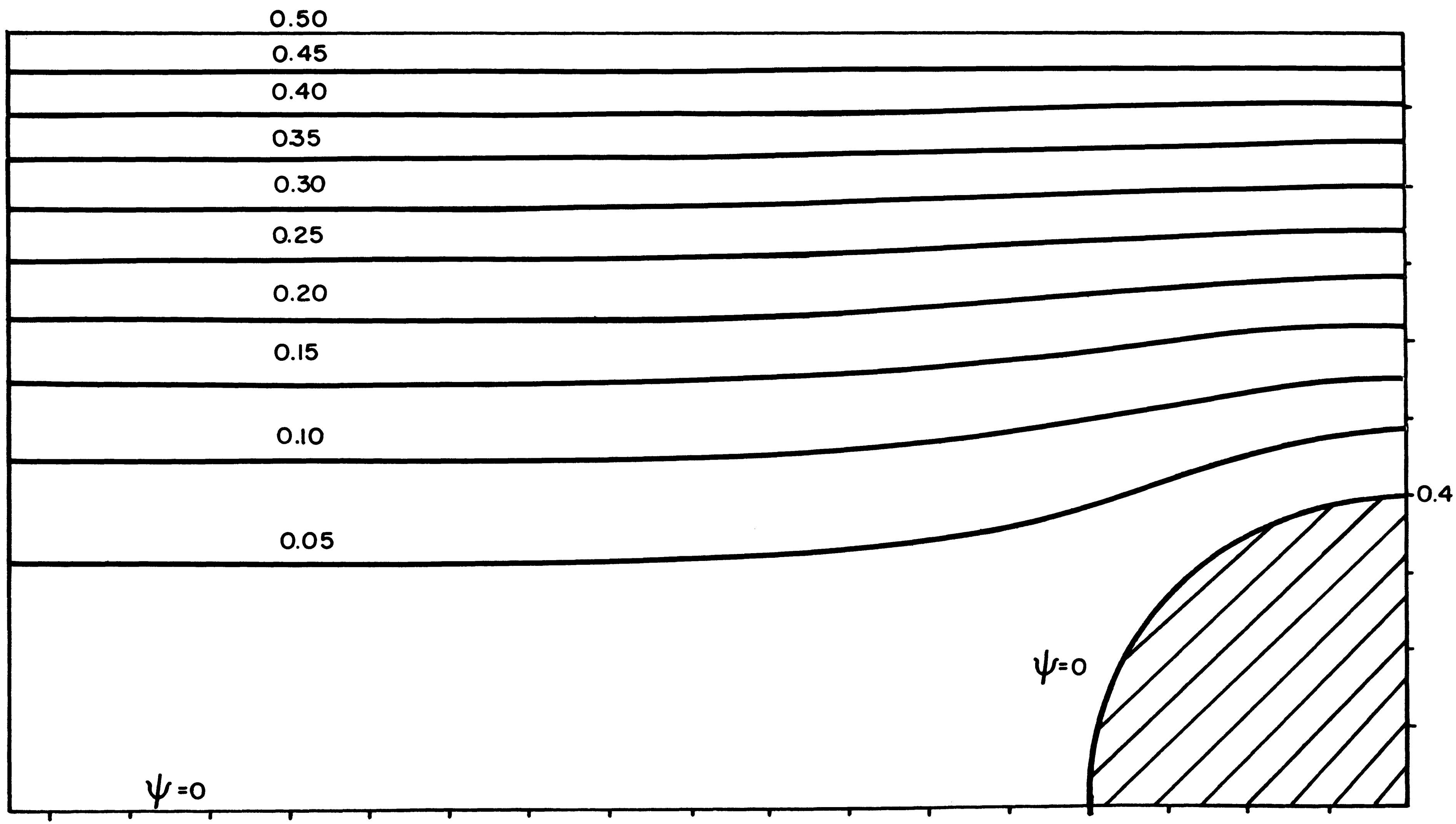

FIG. I FLOW PATTERN FOR IRROTATIONAL FLOW PAST A SPHERE INSIDE A PIPE.

RADIUS OF SPHERE = 0.4

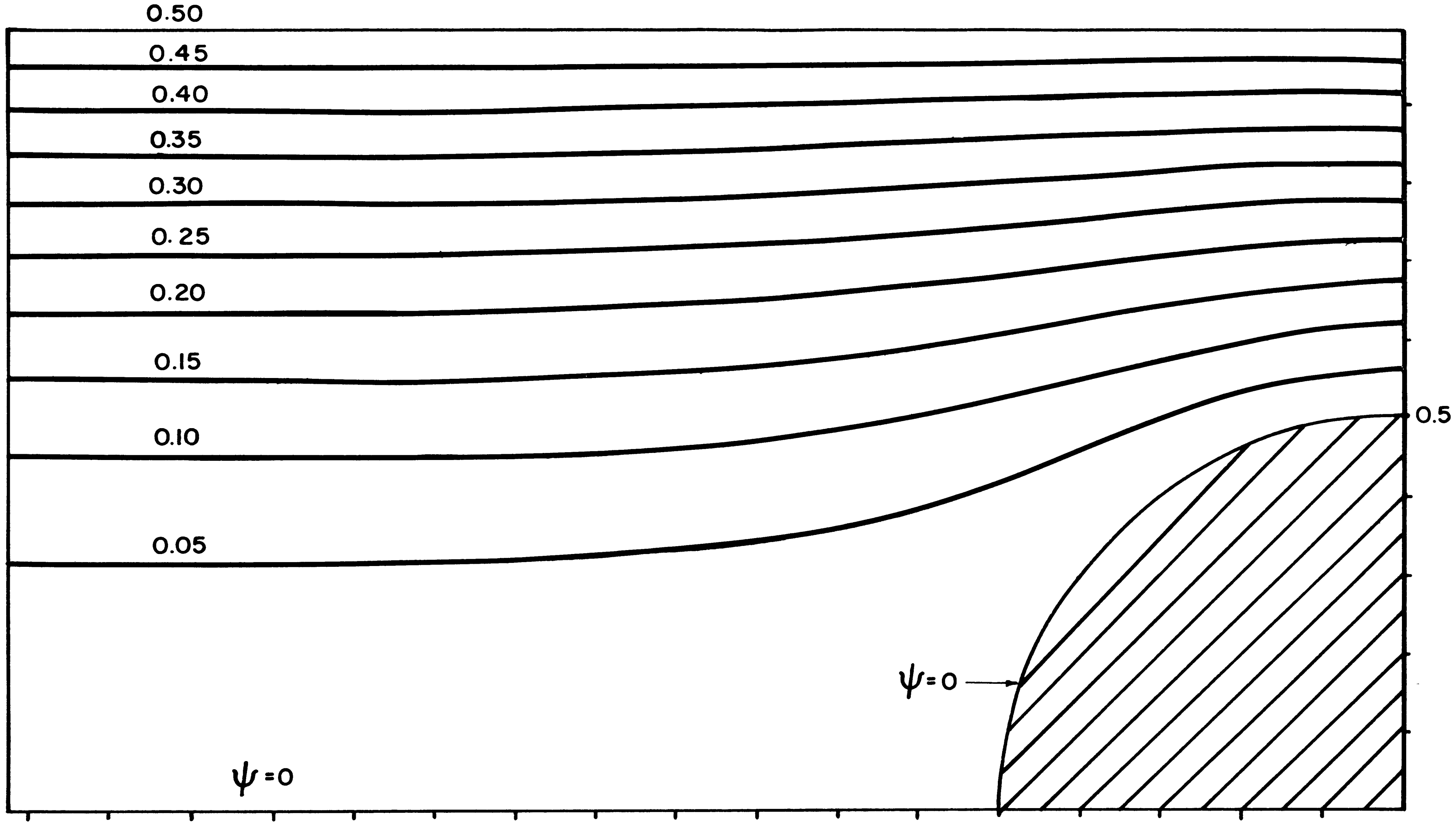

FIG. 2 FLOW PATTERN FOR IRROTATIONAL FLOW PAST A SPHERE INSIDE A PIPE.

RADIUS OF SPHERE = 0.5

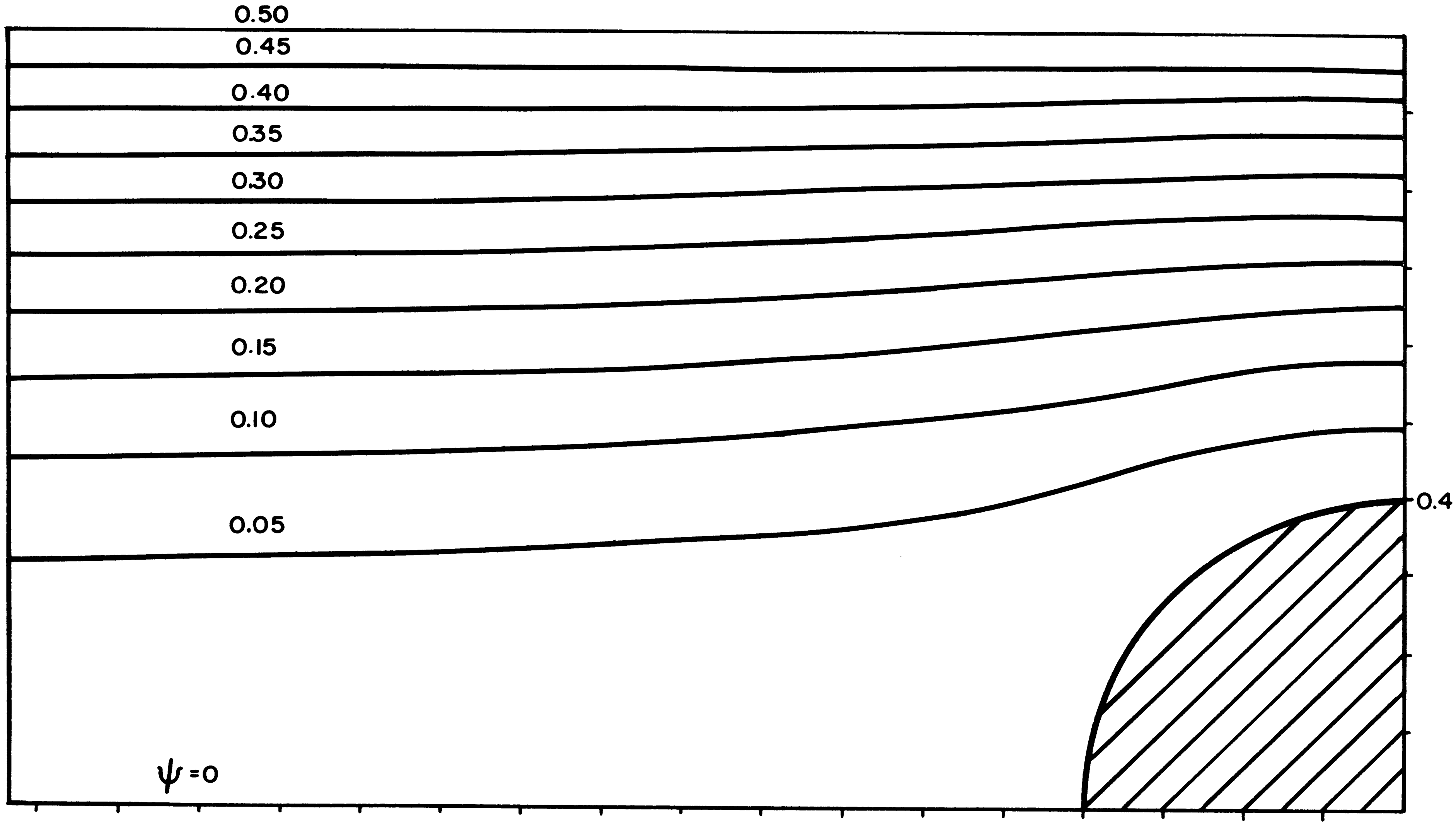

FIG.3 FLOW PATTERN FOR SWIRLING FLOW PAST A SPHERE INSIDE A PIPE.

ROSSBY NUMBER = $\frac{1}{3}$, RADIUS OF SPHERE = 0.4

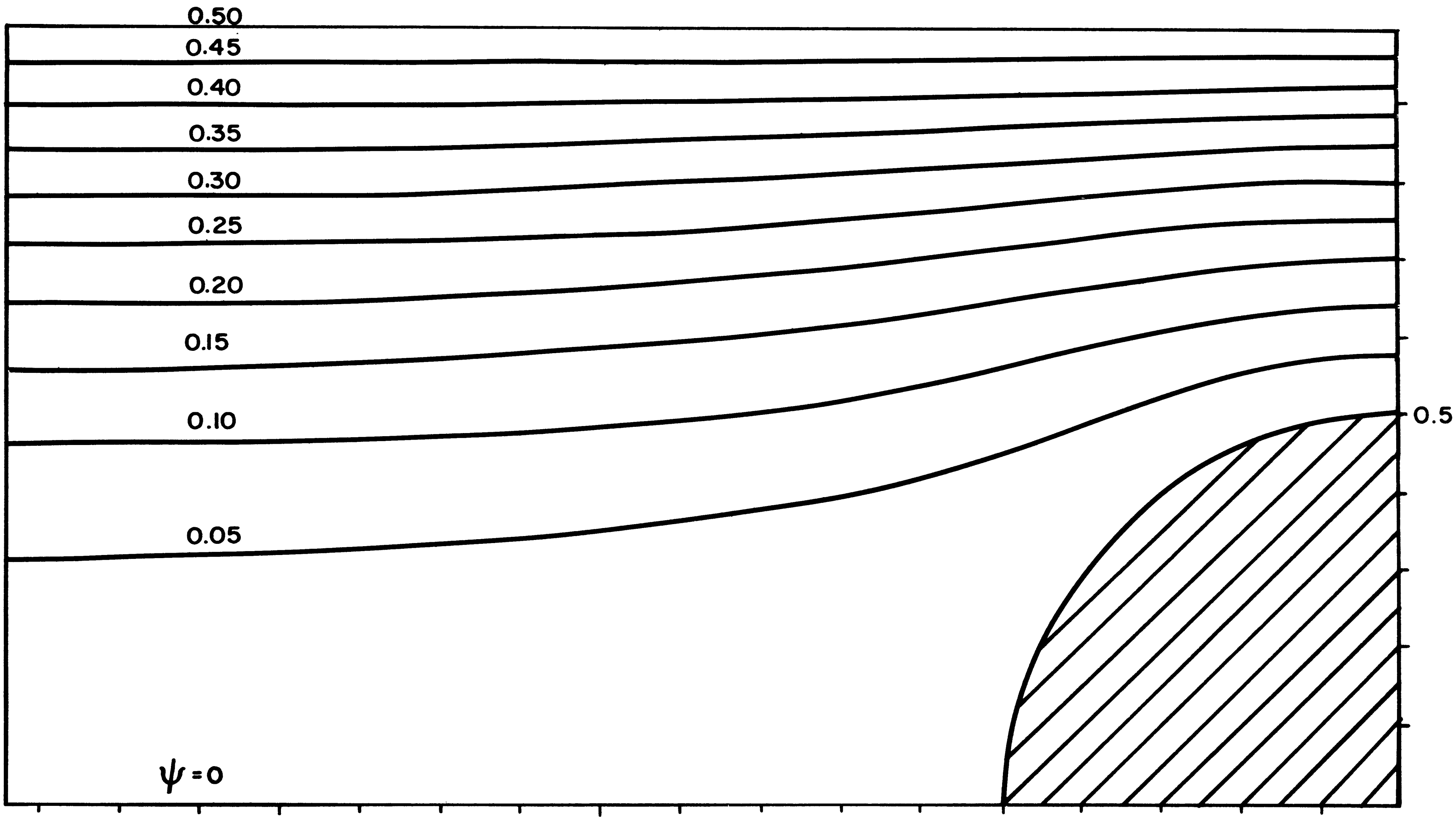

FIG. 4 FLOW PATTERN FOR SWIRLING FLOW PAST A SPHERE INSIDE A PIPE.

ROSSBY NUMBER $= \frac{1}{3}$, RADIUS OF SPHERE $= 0.5$

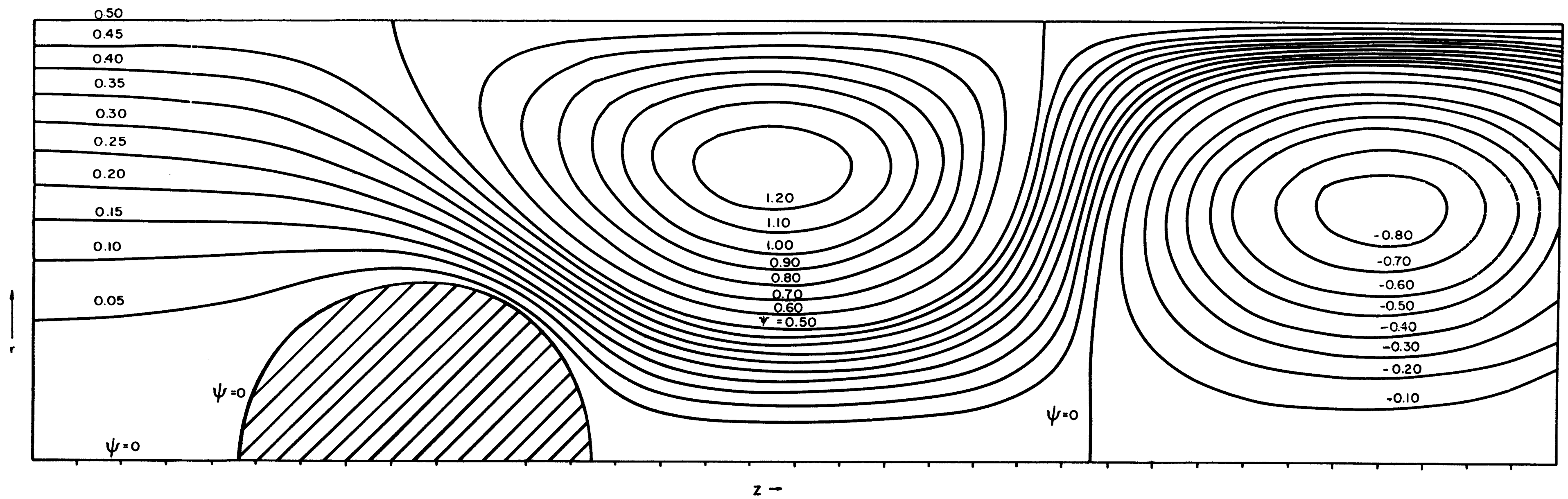

FIG. 5 FLOW PATTERN FOR SWIRLING FLOW PAST A SPHERE INSIDE A PIPE.

ROSSBY NUMBER = $\frac{2}{9}$, RADIUS OF SPHERE = 0.4

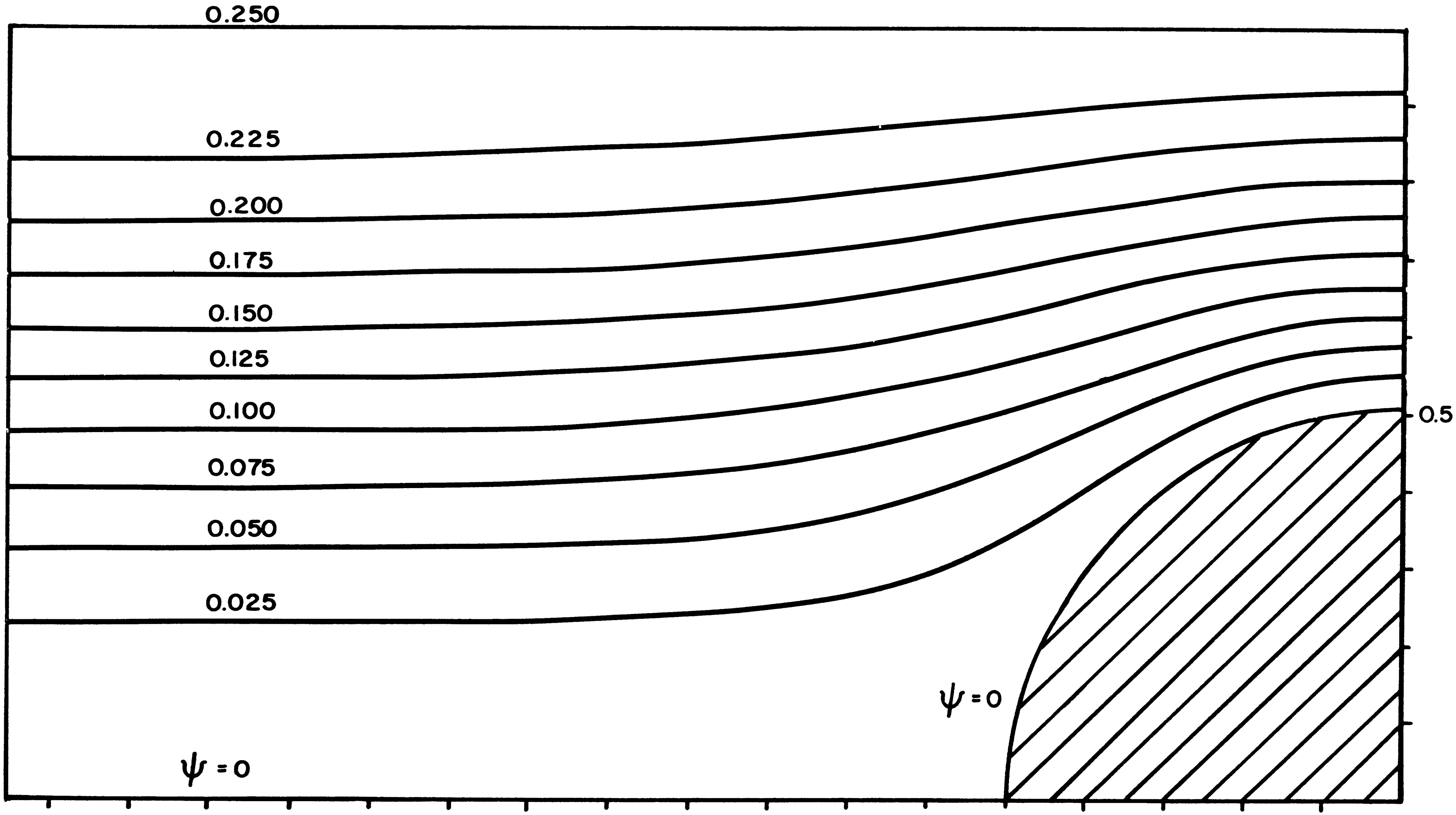

FIG. 6 FLOW PATTERN FOR VORTEX FLOW PAST A SPHERE INSIDE A PIPE.

$W = 1 - r^2$ FAR UPSTREAM, RADIUS OF SPHERE = 0.5

PART THREE. STABILITY OF A REVOLVING FLUID WITH VARIABLE DENSITY IN THE PRESENCE OF A CIRCULAR MAGNETIC FIELD

I. INTRODUCTION

In this part, the stability of an electrically conductive and incompressible fluid between coaxial rotating cylinders in the presence of a radial density gradient as well as a circular magnetic field is studied. Special attention is given to the reles played by the three diffusivities of the fluid, i.e., momentum diffusivity, thermal diffusivity and magnetic diffusivity. The effects of gravity and of the heat generated through viscous and magnetic dissipation are neglected in this study.

When the fluid is homogeneous and no magnetic field is present, it has been proved by many authors (Rayleigh, von Kármán, Sygne) that in the absence of viscosity, the necessary and sufficient condition for stability is that the square of the circulation monotonically increases outwards. Taking viscosity into account, Sygne (1938) has also obtained this condition as a sufficient one. It is therefore often stated that the effect of viscosity in this problem is stabilizing. A consideration, similar to that made by Rayleigh and von Kármán, however, reveals that when the square of the circulation increases monotonically outwards, the diffusive effect of viscosity can actually have a destabilizing tendency. Consider a material ring of the fluid with a radius r. In the steady state, the centrifugal force $\frac{\rho v^2}{r}$, where ρ is density and v the circulatory speed, is balanced by the pressure gradient. When the fluid ring is displaced outwards from r_1 to r_2, whether it would move back (stable) or continue to move outwards (unstable) depends on whether the prevailing pressure gradient is larger or smaller than the centrifugal force of the ring at the new location. The prevailing pressure gradient is $\frac{\rho v_2^2}{r_2}$, where v_2 is the circulatory speed of the steady state at r_2 and is independent of the effect of viscosity on the disturbance. Whereas the centrifugal force of the ring, $\frac{\rho v_1'^2}{r_2}$, where v_1' is the circulatory speed of the ring when it comes to the new location, does depend on the diffusive effect of viscosity. When viscosity is zero, according to Kelvin's circulation theorem, $v_1' = \frac{r_1}{r_2} v_1$, where v_1 is the circulatory speed of the steady state at r_1, and therefore the centrifugal force is $\rho\left(\frac{r_1 v_1}{r_2}\right)^2 \frac{1}{r_2}$ or $\frac{\rho}{r_2^3}(r_1 v_1)^2$. If the square of circulation increases monotonically outwards, $r_2 v_2 > r_1 v_1$ (v_1 and v_2 are positive), then, the difference of pressure gradient and the centrifugal force gives rise to a restoring force $\frac{\rho}{r_2^3}(r_2^2 v_2^2 - r_1^2 v_1^2)$, that tends to push the ring back. While this restoring force is always there as long as the square of the circulation increases monotonically outwards, its magnitude, however, decreases with increasing diffusivity.

This is so because larger diffusivity enables the ring to harmonize better with its new surrounding so that v_1' is closer to v_2 and the magnitude of the restoring force becomes smaller. From this point of view, the flow can therefore be less stable. Even though the flow never really becomes unstable for this case, the destabilizing tendency of the diffusive effect of viscosity is nevertheless there and that the presence of some other field, e.g., temperature field or magnetic field can bring this destabilizing tendency into prominence. Indeed, in a recent paper (1961), Yih has shown that when a temperature gradient is present, the flow can actually become unstable for increasing kinematic viscosity if circulation increases but density decreases outwards. In the present study, it is shown that the same situation arises if a circular magnetic field, which causes instability in the absence of rotation, is present. Actually it arises whenever the combined effect of the temperature field (coupled with the circulation field) and the magnetic field is in favor of instability. What happens then is that as a material ring is displaced, its circulation may harmonize more readily than either the density and/or the magnetic strength along it so that the original cause for stability (the monotonic increase of the square of circulation outwards) can be diminished to such a degree that instability due to the unfavorable temperature and/or magnetic field actually occurs. Since viscosity acts not only as an agent for momentum diffusivity, but also as an agent for dissipation, its capability of playing the dual role, i.e., the role of stabilizing and that of destabilizing simultaneously, is to be expected. In fact, since the dissipation function is, for a given amplitude of the disturbance, directly proportional to viscosity, for sufficiently large viscosity, the disturbance will have to be damped out so that viscosity is always stabilizing when it is sufficiently large.

When a homogeneous quiescent fluid between two nonconductive concentric walls is subjected to a circular magnetic field, it has been shown by Yih (1959a) that, in the absence of magnetic diffusivity, the necessary and sufficient condition for stability is that the quantity $\left(\frac{J'}{\pi r^2}+j_0\right)^2$, where j_0 is the current density passing axially through the fluid, J the line current passing along the axis, r the distance from the axis and $J' = J - \pi j_0 R_1^2$, does not increase outwards. With magnetic diffusivity included, he again obtained this condition as a sufficient one. Thus, the magnetic diffusivity η is always stabilizing whenever the possibility of instability exists, and that for a quiescent fluid, magnetic diffusivity can never be the cause of instability. However, a consideration similar to that regarding viscosity (in the present case, the restoring force is the difference between the pressure gradient and an electromagnetic force, and it is the magnetic strength that is diffused instead of circulation), again reveals that when $\left(j_0+\frac{J'}{\pi r^2}\right)^2$ does not increase outwards, the diffusive effect of η can also have a destabilizing tendency. Therefore, the situation is similar to that discussed in the previous paragraphs in that if either the circulation or the density gradient (coupled with circulation), or their combination is in favor of instability, an increase of magnetic diffusivity, when $\left(j_0+\frac{J'}{\pi r^2}\right)^2$ does not increase outwards, can actually bring about instability. In the present study, the dual role of magnetic diffusivity is also discovered. This is to be expected because magnetic diffusivity is also an agent for dissipation. However, unlike viscosity, which is always stabilizing when it is sufficiently large, magnetic diffusivity need not always stabilize even when it is very large. This is because the rate of dissipation of magnetic energy per unit volume is proportional to the product of diffusivity and the square of current, and for a given amplitude of the velocity disturbance, the perturbation current must eventually decrease as the conductivity decreases indefinitely (or the diffusivity increases indefinitely), so that the product actually decreases with increasing diffusivity so long as the electrical potential difference in the primary configuration is fixed. In other words, when the diffusivity is very large, not only is the perturbation magnetic strength being diffused immediately but also no magnetic energy is dissipated, so that the magnetic field simply does not have any effect on the stability at all. This fact has been shown in the detailed calculation.

Gravity is neglected in this study. The effect of temperature gradient on the motion comes in through the presence of the centripetal acceleration due to rotation of the cylinders. Therefore, to discuss the role played by the thermal diffusivity, circulation field must necessarily be present. As has been mentioned, in the absence of viscosity, the flow of an incompressible fluid is always stable if $\rho\Gamma^2$, where Γ is the circulation, increases with the radial distance. With viscosity included, however, the above condition is by no means a sufficient one, as shown by Yih (1961). What happens is that even when $\rho\Gamma^2$ increases outwards, either the effect of momentum diffusivity (in the case where Γ increases outwards and ρ decreases outwards) or the effect of heat diffusion (in the case where ρ increases outwards and Γ decreases outwards) can make $\rho\Gamma^2$ of a displaced ring larger than that of the new surrounding and therefore the ring tends to move even further outwards. Needless to say, the addition of a magnetic field, unfavorable to stability, would then make the destabilizing effect of the thermal diffusivity even more pronounced. Unlike the other two diffusivities, thermal diffusivity, being non-dissipative, can not simultaneously play the dual role as the other two can. It is either entirely stabilizing or entirely destabilizing.

II. GOVERNING EQUATIONS

With (u, v, w) and (H_r, H_θ, H_z) denoting the components of the velocity and of the magnetic field strength in the directions of the (r, θ, z) coordinate lines, the equations of motion for an incompressible fluid are [see Yih (1959a and b)]

$$\rho\left(\frac{Du}{D\tau} - \frac{v^2}{r}\right) = -\frac{\partial \chi}{\partial r} + \rho\nu\left(\nabla^2 u - \frac{u}{r^2} - \frac{2}{r^2}\frac{\partial v}{\partial \theta}\right) + \frac{\mu}{4\pi}\left(\frac{\mathcal{D} H_r}{\mathcal{D}\tau} - \frac{H_\theta^2}{r}\right), \tag{1}$$

$$\rho\left(\frac{Dv}{D\tau} + \frac{uv}{r}\right) = -\frac{1}{r}\frac{\partial \chi}{\partial \theta} + \rho\nu\left(\nabla^2 v - \frac{v}{r^2} + \frac{2}{r^2}\frac{\partial u}{\partial \theta}\right) + \frac{\mu}{4\pi}\left(\frac{\mathcal{D} H_\theta}{\mathcal{D}\tau} + \frac{H_r H_\theta}{r}\right), \tag{2}$$

$$\rho\frac{Dw}{D\tau} = -\frac{\partial \chi}{\partial z} + \rho\nu\nabla^2 w + \frac{\mu}{4\pi}\frac{\mathcal{D} H_z}{\mathcal{D}\tau}, \tag{3}$$

in which

$$\chi = p + \frac{\mu|\vec{H}|}{8\pi} + \rho\Omega,$$

$$\frac{\mathcal{D}}{\mathcal{D}\tau} = H_r \frac{\partial}{\partial r} + \frac{H_\theta}{r}\frac{\partial}{\partial \theta} + H_z \frac{\partial}{\partial z} \quad ,$$

$$\frac{D}{D\tau} = \frac{\partial}{\partial \tau} + u\frac{\partial}{\partial r} + \frac{v}{r}\frac{\partial}{\partial \theta} + w\frac{\partial}{\partial z} \quad ,$$

$$\nabla^2 = \frac{\partial^2}{\partial r^2} + \frac{1}{r}\frac{\partial}{\partial r} + \frac{1}{r^2}\frac{\partial^2}{\partial \theta^2} + \frac{\partial^2}{\partial z^2} \quad ,$$

and ρ is the density, τ the time, ν the kinematic viscosity, μ the magnetic permeability, and Ω the gravitational potential per unit mass. The equations for the magnetic field are

$$\frac{DH_r}{D\tau} = \frac{\mathcal{D}u}{\mathcal{D}\tau} + \eta\left(\nabla^2 H_r - \frac{H_r}{r^2} - \frac{2}{r^2}\frac{\partial H_\theta}{\partial \theta}\right) , \tag{4}$$

$$\frac{DH_\theta}{D\tau} + \frac{vH_r}{r} = \frac{\mathcal{D}v}{\mathcal{D}\tau} + \frac{H_\theta u}{r} + \eta\left(\nabla^2 H_\theta - \frac{H_\theta}{r^2} + \frac{2}{r^2}\frac{\partial H_r}{\partial \theta}\right) , \tag{5}$$

$$\frac{DH_z}{D\tau} = \frac{\mathcal{D}w}{\mathcal{D}\tau} + \eta\nabla^2 H_z \quad , \tag{6}$$

in which η is the magnetic diffusivity. Neglecting heat generated through viscosity, the equation for heat diffusion is

$$\frac{DT}{D\tau} = k\nabla^2 T \quad , \tag{7}$$

in which T is the temperature and k is the thermal diffusivity. The equations of continuity are

$$\frac{\partial(ru)}{\partial r} + \frac{\partial v}{\partial \theta} + \frac{\partial(rw)}{\partial z} = 0 \quad , \tag{8}$$

and

$$\frac{\partial(rH_r)}{\partial r} + \frac{\partial H_\theta}{\partial \theta} + \frac{\partial(rH_z)}{\partial z} = 0 \quad . \tag{9}$$

III. THE UNDISTURBED STATE

Denoting the radii of the cylinders by r_1 and r_2 (with $r_2 > r_1$), the angular velocities of the cylinders by Ω_1 and Ω_2, the temperature at the walls by T_1 and T_2, the current along the center line (z-axis) of the cylinders by J, and the current density passing between the cylinders by j_0, it can be readily verified that the equations in Section 2 admit the following stationary solution

$$\bar{u}=0, \quad \bar{v}=A_* r+\frac{B_*}{r}, \quad \bar{w}=0, \tag{10}$$

$$\bar{H}_r=0, \quad \bar{H}_\theta=\frac{2J'}{r}+2\pi j_0 r, \quad \bar{H}_z=0, \tag{11}$$

$$\bar{T}=T_1+(T_2-T_1)\frac{\ln r-\ln r_1}{\ln r_2-\ln r_1}, \tag{12}$$

in which

$$A_*=\frac{\Omega_2 r_2^2-\Omega_1 r_1^2}{r_2^2-r_1^2}, \quad B_*=-\frac{(\Omega_2-\Omega_1)r_1^2 r_2^2}{r_2^2-r_1^2} \tag{13}$$

$$J' = J - \pi j_0 r_1^2 , \tag{14}$$

and the equation of state is

$$\bar{\rho} = \rho_1 [1 - \alpha(T - T_1)] , \tag{15}$$

in which ρ_1 is the density of the fluid at the inner wall, α is the coefficient of volume expansion and is assumed to be small in this study.

IV. LINEARIZED EQUATIONS FOR AXISYMMETRIC DISTURBANCE

With the disturbance in the velocity field denoted by (u', v', w'), that in the magnetic field by (h_r, h_θ, h_z) and those in temperature, pressure, and density by θ, p', ρ' respectively, we have

$$u = u', \quad v = \bar{v} + v', \quad w = w',$$

$$H_r = h_r, \quad H = \bar{H}_\theta + h_\theta, \quad H_z = h_z,$$

$$T = \bar{T} + \theta, \quad p = \bar{p} + p', \quad \text{and} \quad \rho = \bar{\rho} + \rho' = \bar{\rho} + (-\alpha \rho_1 \theta).$$

If the above equations are substituted into the governing equations of Section 2, and if all quadratic and higher order terms involving disturbance quantities are dropped, then we obtain the following linearized equations:

$$\rho_1\left(\frac{\partial u'}{\partial \tau} - \frac{2\bar{v}v'}{r} + \alpha\theta\frac{\bar{v}^2}{r}\right) = -\frac{\partial \chi'}{\partial r} + \rho_1\nu\left(\nabla^2 u' - \frac{u'}{r^2}\right) - \mu\left(\frac{J'}{\pi r^2} + j_0\right)h_\theta , \tag{16}$$

$$\rho_1\left(\frac{\partial v'}{\partial \tau} + 2A_* u'\right) = \rho_1\nu\left(\nabla^2 v' - \frac{v'}{r^2}\right) + \mu j_0 h_r , \tag{17}$$

$$\rho_1\frac{\partial w'}{\partial \tau} = -\frac{\partial \chi'}{\partial z} + \rho_1\nu\nabla^2 w' , \tag{18}$$

$$\frac{\partial h_r}{\partial \tau} = \eta\left(\nabla^2 h_r - \frac{h_r}{r^2}\right), \tag{19}$$

$$\frac{\partial h_\theta}{\partial \tau} = \frac{4J'}{r^2}u' - \frac{2B_*}{r^2}h_r + \eta\left(\nabla^2 h_\theta - \frac{h_\theta}{r^2}\right), \tag{20}$$

$$\frac{\partial h_z}{\partial \tau} = \eta \nabla^2 h_z \quad , \tag{21}$$

$$\frac{\partial \theta}{\partial \tau} + u\frac{\partial \bar{T}}{\partial r} = k\nabla^2\theta, \tag{22}$$

and

$$\frac{\partial (ru')}{\partial r} + \frac{\partial (rw')}{\partial z} = 0 . \tag{23}$$

From the form of equations (19) and (21) we can conclude that h_z and h_r will be damped out if they are not initially everywhere zero (see Yih 1959b). Eliminating χ' from equations (16) and (18), we have

$$\rho_1\nu\left(\nabla^2-\frac{1}{r^2}-\frac{1}{\nu}\frac{\partial}{\partial\tau}\right)\left(\frac{\partial w'}{\partial r}-\frac{\partial u'}{\partial z}\right)=\rho_1\left(\frac{2\bar{V}}{r}\frac{\partial v'}{\partial z}-\alpha\frac{\bar{V}^2}{r}\frac{\partial\theta}{\partial z}\right)$$

$$-\mu\left(\frac{J'}{\pi r^2}+j_0\right)\frac{\partial h_\theta}{\partial z} \quad . \tag{24}$$

We assume, after Taylor,

$$(u', v', \theta, h_\theta)=[u_1(r), v_1(r), \theta_1(r), h_1(r)]\cos\lambda z\, e^{\sigma\tau},$$

$$w'=w_1(r)\sin\lambda z\, e^{\sigma\tau}, \tag{25}$$

in which λ is the wave number for the z direction. The equation of continuity (23) then becomes

$$rDu_1+u_1+\lambda r w_1(r)=0 \ , \tag{26}$$

and equations (24), (17), (20), and (22) become

$$\left(L-\lambda^2-\frac{\sigma}{\nu}\right)\left(L-\lambda^2\right)u_1=\frac{\lambda^2}{\nu}\left(\frac{2\bar{V}}{r}v_1-\alpha\frac{\bar{V}^2}{r}\theta_1\right)$$

$$-\frac{\lambda^2\mu}{\rho\nu}\left(\frac{J'}{\pi r^2}+j_0\right)h_1 \ , \tag{27}$$

$$\left(L-\lambda^2-\frac{\sigma}{\nu}\right)v_1=\frac{2A_*}{\nu}u_1 \;, \tag{28}$$

$$\left(L-\lambda^2-\frac{\sigma}{\eta}\right)h_\theta=-\frac{4J'}{\eta}\frac{u_1}{r^2} \;, \tag{29}$$

$$\kappa\left(L'-\lambda^2-\frac{\sigma}{\kappa}\right)\theta=u_1\frac{d\overline{T}}{dr} \;, \tag{30}$$

in which

$$D=\frac{d}{dr}\;, \qquad L=D\left(D+\frac{1}{r}\right)=D\left\{\frac{1}{r}D(r\quad)\right\},$$

$$L'=\frac{d^2}{dr^2}+\frac{1}{r}\frac{d}{dr}\;.$$

The boundary conditions for u_1 and v_1 are

$$u_1=Du_1=v_1=0 \quad \text{at } r=r_1 \text{ and } r_2 \;. \tag{31a}$$

The boundary conditions for θ are, if the walls are assumed much more conductive than the fluid,

$$\theta=0 \quad \text{at } r=r_1 \text{ and } r_2 \;. \tag{31b}$$

The simplest realistic boundary conditions for h is that which corresponds to zero electrical conductivity of the walls, that is, to $j_r = 0$. But

$$j_r = \frac{1}{r}\frac{\partial h_z}{\partial \theta} - \frac{\partial h_\theta}{\partial z} = -\frac{\partial h_\theta}{\partial z}, \qquad \text{(for axisymmetry)}$$

So the boundary condition for h are

$$h = 0 \quad \text{at } r = r_1 \text{ and } r_2 \tag{31c}$$

for non-conducting walls.

The homogeneous differential system consisting of (27), (28), (29), (30) and the boundary conditions (31a), (31b), (31c) define an eigenvalue problem.

V. THE CASE OF SMALL SPACING

If $r_2 - r_1 \ll r_1$, then we need not distinguish between D^2 and L and if the dimensionless quantities

$$\left.\begin{aligned} &\xi = \frac{r-r_1}{r_2-r_1}\ , \quad k=\lambda(r_2-r_1)\ , \\ &(u_2, v') = \left(\frac{u_1}{r_1\Omega_1}\ , \ \frac{v_1}{r_1\Omega_1}\right), \\ &\theta' = \alpha\theta_1\ , \quad \text{and} \quad h' = \frac{h_1}{r_1 j_0}\ , \end{aligned}\right\} \tag{32}$$

are introduced, equations (27), (28), (29) and (30) become

$$\begin{aligned}\left(D^2-k^2-\frac{\sigma R'}{\Omega_1}\right)(D^2-k^2)u_2 &= 2k^2R'\omega v' - k^2\omega^2R'\frac{r}{r_1}\theta' \\ &\quad -k^2R'N_1\left(1-2\frac{r_2-r_1}{r_1}\frac{J'}{J}\xi\right)h'\ ,\end{aligned} \tag{33}$$

$$\left(D^2-k^2-\frac{\sigma R'}{\Omega_1}\right)v_1' = 2AR'u_2\ , \tag{34}$$

$$\left(D^2-k^2-\frac{\sigma(r_2-r_1)^2}{\eta}\right)h' = N_2u_2\ , \tag{35}$$

$$\left(D^2 - k^2 - \frac{\sigma(r_2-r_1)^2}{\eta}\right)\theta' = \alpha \frac{dT}{dr} r_1 \, P\acute{e} \, u_2 , \qquad (36)$$

in which

$$\left.\begin{aligned} &\omega = \frac{\bar{V}}{r\Omega_1} , \quad A = \frac{A_*}{\Omega_1} , \quad B = \frac{B_*}{\Omega_1} , \\ &R' = \frac{(r_2-r_1)^2\Omega_1}{\nu} , \quad N_1 = \frac{\mu \dot{j}_0 J}{\rho \Omega_1^2 \pi r_1^2} , \quad N_2 = -\frac{4J'\Omega_1(r_2-r_1)^2}{\eta \dot{j}_0 r_1^2} , \\ &P\acute{e} = \frac{\Omega_1 (r_2-r_1)^2}{k} . \end{aligned}\right\} \qquad (37)$$

Now, since

$$\omega = A + B\left[1 + (r_2-r_1)\xi/r_1\right]^{-2} ,$$

we can write, with higher powers in $(r_2 - r_1)/r_1$ neglected,

$$\omega = 1 + \alpha'\xi \quad \text{and} \quad \alpha' = \frac{\Omega_2}{\Omega_1} - 1 . \qquad (38)$$

Also,

$$\frac{dT}{dr} = \frac{T_2 - T_1}{r_2 - r_1}\left(1 - \frac{r_2-r_1}{r_1}\xi\right) = \beta\left(1 - \frac{r_2-r_1}{r_1}\xi\right) ,$$

so that, for $r_2 - r_1 \ll r_1$,

$$\frac{dT}{dr} = \beta = \frac{T_2 - T_1}{r_2 - r_1} . \qquad (39)$$

If now (38) and (39) are substituted in (33) and (36) and by invoking the principle of exchange of stability, we obtain

$$(D^2-k^2)^2 u_2 = 4k^2R'^2A(1+\alpha'\xi)V_2 - k^2R'\alpha\beta P\acute{e}(1+2\alpha'\xi + \alpha'^2\xi^2)\theta_2 - k^2R'G\left(1-2\frac{r_2-r_1}{r_1}\frac{J'}{J}\xi\right)h_2 , \quad (40)$$

$$(D^2-k^2)V_2 = u_2 \quad (41)$$

$$(D^2-k^2)h_2 = u_2 \quad (42)$$

$$(D^2-k^2)\theta_2 = u_2 \quad (43)$$

with

$$\frac{V'}{2AR'} = V_2, \ \frac{h'}{N_2} = h_2, \ \frac{\theta'}{\alpha\beta r_1 P\acute{e}} = \theta_2, \text{ and } G = N_1N_2 \quad (44)$$

The boundary conditions are

$$u_2 = Du_2 = 0 \ \text{ at}$$

$$v_2 = h_2 = \theta_2 = 0 \quad at\ \xi = 0\ and\ 1\ . \tag{46}$$

Since the differential equations and the boundary conditions are identical for v_2, θ_2, and h_2, we conclude that

$$v_2 = \theta_2 = h_2\ . \tag{47}$$

Thus the differential system that we have to solve is

$$(D^2 - K^2)^2 u_2 = -K^2 T(1 + P_2\xi + P_3\xi^2) v_2\ , \tag{48}$$

$$(D^2 - K^2) v_2 = u_2\ , \tag{49}$$

with the boundary conditions

$$u_2 = Du_2 = v_2 = 0 \quad at\ \xi = 0\ and\ 1, \tag{50}$$

in which

$$T = -(C - D - E), \tag{51}$$

$$P_2 = C\alpha' - 2D\alpha' + 2E\frac{r_2 - r_1}{r_1}\frac{J'}{J}\ , \tag{52}$$

$$P_3 = -\frac{D\alpha'^2}{C-D-E} , \tag{53}$$

$$C = 4R'^2 A, \tag{54}$$

$$D = R'\alpha\beta r_1 P\acute{e} , \tag{55}$$

and

$$E = R'G . \tag{56}$$

The above differential system will be solved by the method of Chandrasekhar (1953) in the next section, in which the critical Taylor number T, which is the least of all the lowest eigenvalues corresponding to different values of wave number k, will be obtained as a function of P_2 and P_3 in the form of tables and curves. (See section 6).

From equations (51), (52) and (53), we obtain

$$C = \left[-P_2 T + \frac{2P_3 T}{\alpha'} - 2T\left(1-\frac{P_3}{\alpha'^2}\right)\frac{r_2-r_1}{r_1}\frac{J'}{J}\right] \Big/ \left(\alpha'^4 + 2\frac{r_2-r_1}{r_1}\frac{J'}{J}\right), \tag{54a}$$

$$D' = \frac{D}{\sqrt{|C|}} = \frac{P_3 T}{\alpha'^2 \sqrt{|C|}} , \tag{55a}$$

$$E' = \frac{E}{\sqrt{|C|}} = \frac{(T+C-D)}{\sqrt{|C|}} . \tag{56a}$$

Note that each of the C, D', E' contains only one of the diffusivities. Indeed

$$C = \frac{4(r_2-r_1)^4 \Omega_1 A}{\nu^2} , \tag{54b}$$

$$D' = \frac{\alpha\beta r_1 \Omega_1 (r_2-r_1)^2}{2\sqrt{|A|}\, k} , \tag{55b}$$

$$E' = -\frac{2\mu J J'(r_2-r_1)^2}{\rho\pi\sqrt{|A|}\, r_1^4 \Omega_1 \eta} . \tag{56b}$$

Since T is a function of P_2 and P_3, therefore, for fixed values of $\frac{\Omega_2}{\Omega_1}$ and $\frac{r_2-r_1}{r_1}\frac{J'}{J}$, which characterize some particular circulation and magentic fields, equations (54a), (55a), and (56a) take the following parametric form

$$C = f_1(P_2,P_3), \quad D' = f_2(P_2,P_3) \text{ and } E' = f_3(P_2,P_3), \tag{57}$$

and therefore represent a surface in the C-D'-E' space. Curves on planes cutting the surface and perpendicular to either of the three coordinates are obtained in Section 7, with preceding discussions of the roles played by the three diffusivities.

VI. SOLUTION FOR SMALL SPACING BY THE METHOD OF CHANDRASEKHAR

For clarity, equations (48), (49) and (50) are rewritten in the following forms:

$$(D^2-K^2)^2 U_2 = -K^2 T(1+P_2\xi+P_3\xi^2)V_2 \tag{48}$$

$$(D^2-K^2)V_2 = U_2 \tag{49}$$

$$U_2 = DU_2 = V_2 = 0 \quad \text{at } \xi=0 \text{ and } 1. \tag{50}$$

Since v_2 has to vanish at $\xi = 0$ and 1, we shall expand it in a sine series of the form

$$V_2 = \sum_{n=1}^{\infty} C_n \sin n\pi\xi. \tag{58}$$

Substituting this into equation (48), we have

$$(D^2-K^2)^2 U_2 = -K^2 T(1+P_2\xi+P_3\xi^2)\sum_{m=1}^{\infty} C_m \sin m\pi\xi. \tag{59}$$

The general solution of equation (59) can be written in the form

$$
\begin{aligned}
u_2 = -k^2 T \sum_{m=1}^{\infty} \frac{C_m}{(m^2\pi^2+k^2)^2} \Big\{ & A_1^{(m)} \cosh k\xi + B_1^{(m)} \sinh k\xi \\
& + A_2^{(m)} \xi \cosh k\xi + B_2^{(m)} \xi \sinh k\xi + \Big[1 + P_2 \xi \\
& + P_3 \Big(\xi^2 + \frac{4}{m^2\pi^2+k^2} - \frac{24 m^2\pi^2}{(m^2\pi^2+k^2)^2} \Big) \Big] \sin m\pi\xi \\
& + \frac{4P_3 m\pi}{m^2\pi^2+k^2} \cos m\pi\xi + \frac{8m\pi P_3}{m^2\pi^2+k^2} \xi \cos m\pi\xi \Big\}
\end{aligned}
\tag{60}
$$

where the constants of integration $A_1^{(m)}$, $B_1^{(m)}$, $A_2^{(m)}$ and $B_2^{(m)}$ are determined by the boundary conditions that $u_2 = Du_2 = 0$ at $\xi = 0$ and 1. They are the following

$$
\left.
\begin{aligned}
& A_1^{(m)} = -\frac{4m\pi}{M}, \quad M = m^2\pi^2 + k^2, \\
& A_2^{(m)} = \frac{1}{k^2 - \sinh^2 k} \Big\{ (-1)^{m+1} \frac{4m\pi k}{M} (P_2 + 2P_3)(\sinh k \\
& \quad + k\cosh k) - A_1^{(m)} (k^2 + k\cosh k \sinh k) \\
& \quad + \Big[1 + P_3 \Big(\frac{12}{M} - \frac{24 m^2\pi^2}{M^2} \Big) \Big] m\pi \sinh^2 k \\
& \quad - (-1)^{m+1} \Big[1 + P_2 + P_3 \Big(1 + \frac{12}{M} - \frac{24 m^2\pi^2}{M^2} \Big) \Big] \\
& \quad m\pi k \sinh k \Big\},
\end{aligned}
\right\}
\tag{61}
$$

$$\left.\begin{aligned} B_1^{(m)} &= -\frac{1}{K}\left\{A_2^{(m)} + \left[1 + P_3\left(\frac{12}{M} - \frac{24m^2\pi^2}{M^2}\right)\right]m\pi\right\}, \\ B_2^{(m)} &= -\frac{1}{\sinh K}\left\{A_1^{(m)}\cosh K + B_1^{(m)}\sinh K + A_2^{(m)}\cosh K \right. \\ &\left. + \frac{4P_2 m\pi}{M}(-1)^m + \frac{8m\pi P_3}{M}(-1)^m\right\}. \end{aligned}\right\}$$

Now, substituting for v_2 and u_2 from equations (58) and (60) in equation (49), we obtain

$$\begin{aligned} \sum_{n=1}^{\infty} C_n(n^2\pi^2 + K^2)\sin n\pi\xi &= K^2 T \sum_{m=1}^{\infty} \frac{C_m}{(m^2\pi^2+K^2)}\left\{A_1^{(m)}\cosh K\xi \right. \\ &+ B_1^{(m)}\sinh K\xi + A_2^{(m)}\xi\cosh K\xi + B_2^{(m)}\xi\sinh K\xi \\ &+ \left[1 + P_2\xi + P_3\left(\xi^2 + \frac{4}{M} - \frac{24m^2\pi^2}{M^2}\right)\right]\sin m\pi\xi \\ &\left. + \frac{4P_2 m\pi}{M}\cos m\pi\xi + \frac{8m\pi P_3}{M}\xi\cos m\pi\xi\right\}. \end{aligned} \tag{62}$$

Multiplying this equation by $\sin(n\pi\xi)$ and integrating over the range of ξ, we obtain

$$\sum_{m=1}^{\infty}\Big[\frac{n\pi}{n^2\pi^2+k^2}\Big\{[1+(-1)^{n+1}\cosh k]A_1^{(m)}+[(-1)^{n+1}\sinh k]B_1^{(m)}$$

$$+(-1)^{n+1}\Big[\cosh k-\frac{2k}{n^2\pi^2+k^2}\sinh k\Big]A_2^{(m)}+\Big[(-1)^{n+1}\sinh k \tag{63}$$

$$-\frac{2k}{n^2\pi^2+k^2}\{1+(-1)^{n+1}\cosh k\}\Big]B_2^{(m)}\Big\}+\frac{1}{2}\delta_{nm}$$

$$+P_2X_{nm}+P_3Y_{nm}-\frac{1}{2}(n^2\pi^2+k^2)^3\frac{\delta_{nm}}{k^2T}\Big]G_m=0,$$

where

$$G_m=C_m(m^2\pi^2+k^2)^{-2}, \tag{64}$$

$$\left.\begin{aligned}
X_{nm}&=\begin{cases}\frac{1}{4} & \text{if } m=n,\\ 0 & \text{if } m+n \text{ is even and } m\neq n,\\ \frac{4mn}{n^2-m^2}\Big\{\frac{2}{m^2\pi^2+k^2}-\frac{1}{\pi^2(n^2-m^2)}\Big\} & \text{if } m+n \text{ is odd;}\end{cases}\\
Y_{nm}&=\begin{cases}\frac{1}{6}-\frac{1}{4m^2\pi^2}-\frac{12m^2\pi^2}{(m^2\pi^2+k^2)^2} & \text{if } m=n,\\ -\frac{4mn}{(n^2-m^2)}\Big\{\frac{2}{m^2\pi^2+k^2}-\frac{1}{\pi^2(n^2-m^2)}\Big\} & \text{if } m+n \text{ is even and } m\neq n,\\ \frac{4mn}{n^2-m^2}\Big\{\frac{2}{m^2\pi^2+k^2}-\frac{1}{\pi^2(n^2-m^2)}\Big\} & \text{if } m+n \text{ is odd.}\end{cases}
\end{aligned}\right\} \tag{65}$$

Equation (63) represents a system of linear homogeneous equations on the G_m's. Consequently, if the G_m's are not all to vanish identically, it is necessary that the determinant of the system vanishes, i.e.,

$$\Bigg| \frac{n\pi}{n^2\pi^2+k^2}\Big\{\left[1+(-1)^{n+1}\cosh k\right]A_1^{(m)}+\left[(-1)^{n+1}\sinh k\right]B_1^{(m)}$$

$$+(-1)^{n+1}\left[\cosh k-\frac{2k}{n^2\pi^2+k^2}\sinh k\right]A_2^{(m)}+\Big[(-1)^{n+1}\sinh k$$

$$-\frac{2k}{n^2\pi^2+k^2}\left(1+(-1)^{n+1}\cosh k\right)\Big]B_2^{(m)}\Big\}+\frac{1}{2}\delta_{nm}+P_2X_{nm} \tag{66}$$

$$+P_3Y_{nm}-\frac{1}{2}(n^2\pi^2+k^2)^3\frac{\delta_{nm}}{k^2T}\Bigg|=0$$

Equation (66) is the required characteristic equation for T. Numerical results are given in Tables (1) to (8), and also in Figure 9. The order of approximation listed in the tables is the order of the determinant which is set equal to zero in the determination of T. For each set of values P_2 and P_3, values of k were chosen (by trial and error) in the range in which T (as a function of k) attains its minimum value. Values of k are also listed in the tables.

VII. DISCUSSIONS AND CONCLUSIONS

For the discussion of the following graphs, it is useful to remember the following:

(I) For C (Note that C is the first letter of the word circulation):

(1) It contains kinematic viscosity in the denominator, therefore, small C corresponds to large momentum diffusivity.

(2) Positive C corresponds to the case where circulation increases monotonically outwards. It therefore corresponds to stable circulation field.

(3) Positive C is consistent only with $\frac{\Omega_2}{\Omega_1} > 0$, and negative C is consistent only with $\frac{\Omega_2}{\Omega_1} < 1$.

(II) For D' (D is the first letter of density):

(1) It contains thermal diffusivity in the denominator. Therefore, small D corresponds to large thermal diffusivity.

(2) Positive D' corresponds to the case where temperature increases outwards and consequently density decreases outwards. It therefore corresponds to temperature fields unfavorable to stability.

(III) For E' (E is the first letter of electromagnetism):

(1) It contains magnetic diffusivity in the denominator. Therefore, small E corresponds to large magnetic diffusivity.

(2) Positive E' corresponds to $\pi \mathcal{J}_0 r_1^2 - J > 0$. It therefore corresponds to magnetic fields unfavorable to stability.

(3) Positive E' is consistent only with negative $\frac{r_2-r_1}{r_1}\frac{J'}{J}$ and negative E' is consistent only with positive $\frac{r_2-r_1}{r_1}\frac{J'}{J}$.

(IV) Any one curve in the graphs represents marginal stability for the specific parameter associated with that curve. It divides the plane of the curve into two regions. The region that has the origin in its interior is the stable region, and the other region is the unstable one. (See a remark on page 78).

Figure 1 corresponds to the case where only circulation and density fields are present. This case has been studied by Yih (1961). However, in his study, the two cylinders are assumed to rotate in the same directions and that Ω_2/Ω_1 is approximately equal to one so that the square of the quantity $\left(\frac{\Omega_2}{\Omega_1}-1\right)$ can be neglected in comparison with itself. In the present study, no such assumption is made. The graphs show that for positive C, and for a given value of Ω_2/Ω_1, there is a region in which the flow is destabilized as the viscosity is increased, i.e., the region to the right of the point of relative minimum of the ordinate of the curve for the particular value of Ω_2/Ω_1 considered. Outside of this region, viscosity is always stabilizing. Thus, the dual role of viscosity is clearly seen. Thermal diffusivity is entirely stabilizing for positive C. For negative C, the stability region is to the right of each curve, and the instability region to the left. Viscosity is entirely stabilizing. Thermal diffusivity is either entirely stabilizing or entirely destabilizing according as D' is positive or negative. The region below the dashed line curve is the region of absolute stability, i.e., stable for whatever values of Ω_2/Ω_1. This curve is obtained by putting the critical Taylor number equal to zero, the minimum of the eigenvalues of the differential system. It corresponds to P_2 equal to infinity. Any point below the dashed line curve corresponds to negative Taylor number, and therefore smaller than the critical one.

Figure 2 corresponds to the case where magnetic field, unfavorable to stability, is present. It is seen that for positive C, all curves move downwards (compared with Figure 1) toward the horizontal axis, showing a reduction of stability region. Also, along a line of constant D', when viscosity increases, one moves into the instability region sooner and moves out later than in Figure 1 for the same constant D'. Also, curves are closer to one another, showing that the importance of the parameter Ω_2/Ω_1 is overshadowed by the magnetic field. A similar situation exists for negative C. The situation becomes even more pronounced when the fluid is magnetically less diffusive, as is shown in Figure 3. Dashed line curves in Figures 2 and 3 have the same meaning as that in Figure 1.

The dual role of magnetic diffusivity is shown in Figure 4. In the second quadrant of that figure, magnetic fields are favorable to stability and density fields are unfavorable (coupled with a favorable circulation field). It is seen that for some values of $\frac{d}{r_1}\frac{J'}{J}$, where $d = r_2 - r_1$, (specifically for $\frac{d}{r_1}\frac{J'}{J} > 1$ in that figure), if one moves along a line of constant D' in the direction of increasing magnetic diffusivity, one moves from the stability region into the instability region and then again to the stability region. For other values of $\frac{d}{r_1}\frac{J'}{J}$ $(0 < \frac{d}{r_1}\frac{J'}{J} < 1.0)$, however, the magnetic diffusivity is entirely destabilizing, even when it approaches infinity. This situation is rather different from that regarding viscosity. Viscosity is always stabilizing when it is very large, but magnetic diffusivity is not always so. The fact that all the curves in Figure 4 meet at the same point that marks the marginal stability in the absence of a magnetic field indicates that when magnetic diffusivity becomes very large, its effect becomes nil. In the first quadrant, both magnetic and density fields are unfavorable, and both diffusivities are stabilizing, whereas in quadrant 4, density field is favorable and magnetic field is unfavorable and, as a result, the thermal diffusivity is entirely destabilizing and magnetic diffusivity is stabilizing. The two regions outside the two parallel dashed lines are regions of absolute stability in the sense that they are stable for whatever values of $\frac{d}{r_1}\frac{J'}{J}$.

After all these discussions, the rest of the figures are really self-explanatory. Figure 5, Figure 6, and Figure 7 are for the case where only magnetic and circulation fields are present. The reduction of stability region when one of the field becomes less favorable, is clearly seen. The dual role of magnetic diffusivity appears again in the third quadrant of Figure 7.

Remark: In all the figures except Figure 4, the origin is a point that corresponds to a fluid with infinite viscosity. In Figure 4, it corresponds to an electrically non-conductive fluid, subjected to no temperature gradient and to a circulation field favorable to stability. Therefore, in all the figures the region that has the origin in its interior is a region of stability.

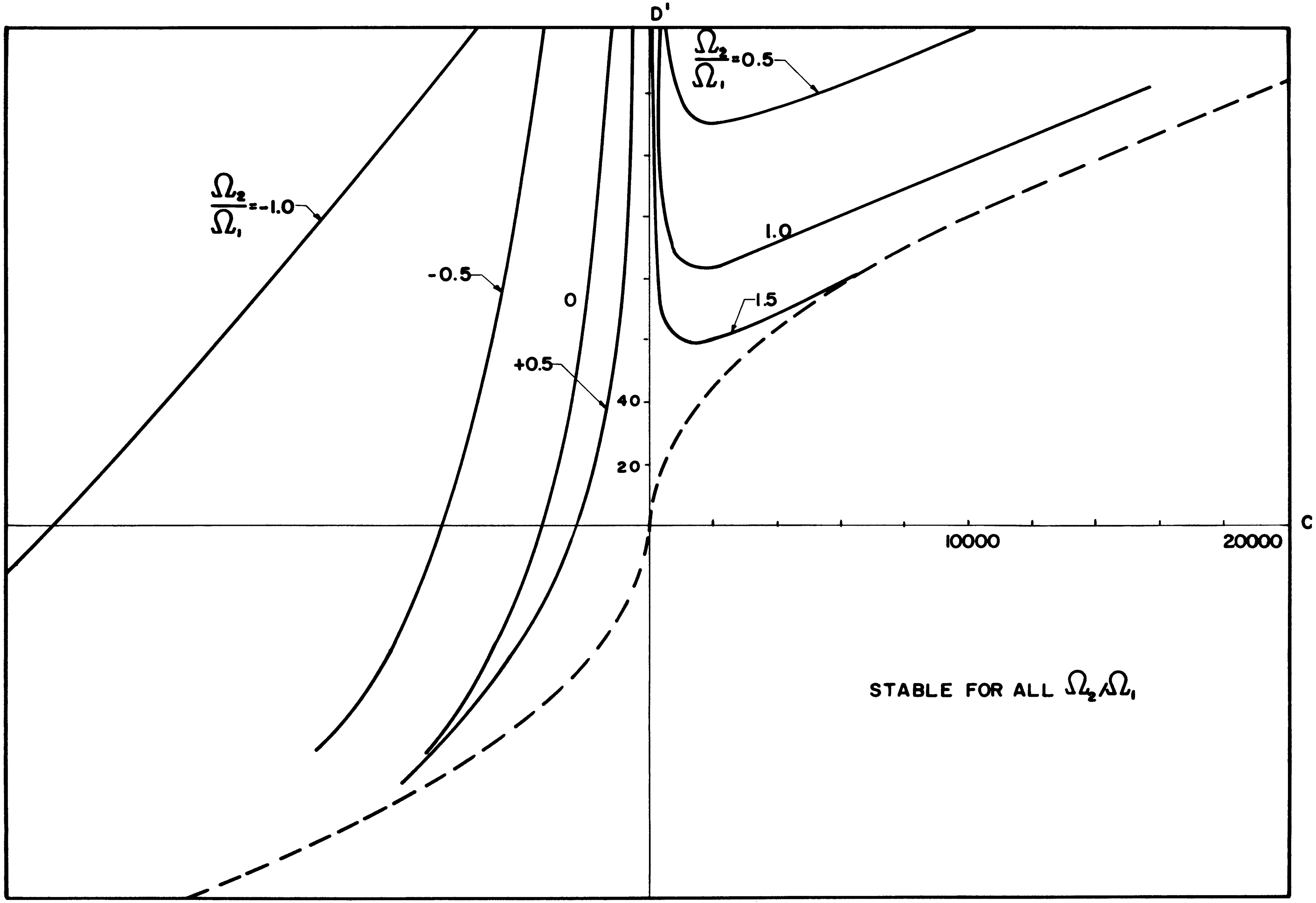

FIG. I MARGINAL STABILITY CURVES FOR E' = 0

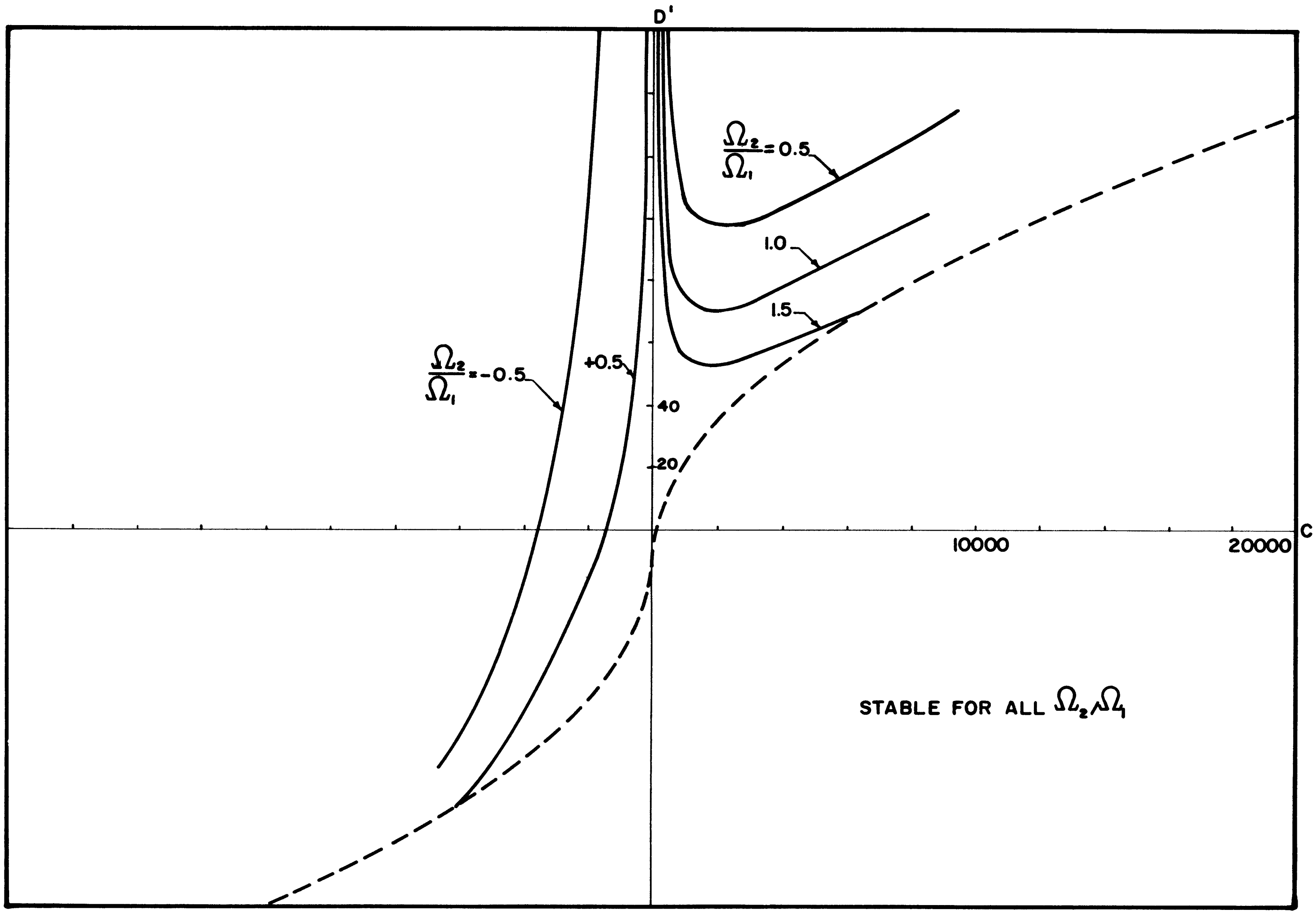

FIG. 2 MARGINAL STABILITY CURVES FOR $E' = 10$ AND $\frac{d}{r_1}\frac{J'}{J} = -0.30$

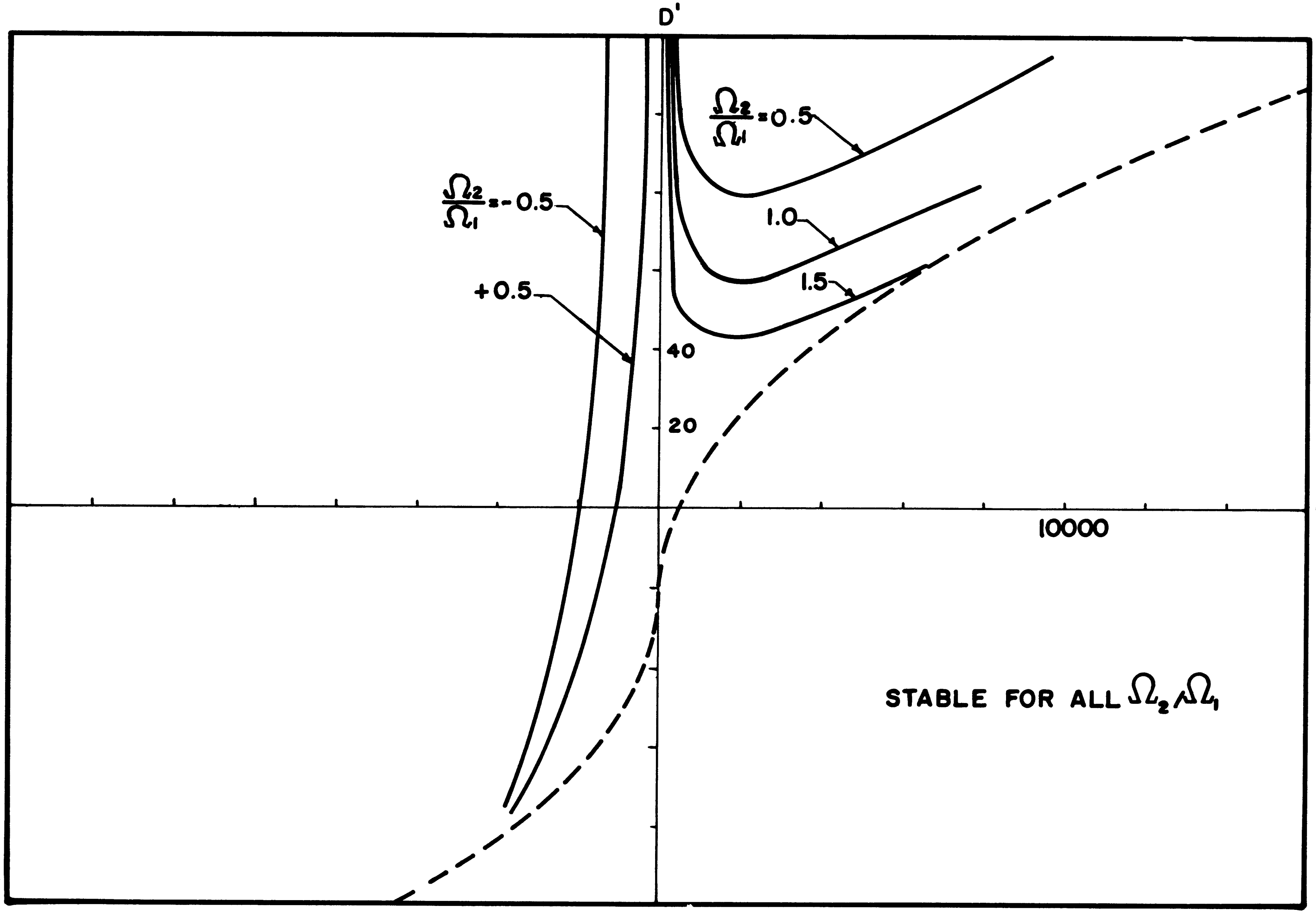

FIG.3 MARGINAL STABILITY CURVES FOR E' = 20

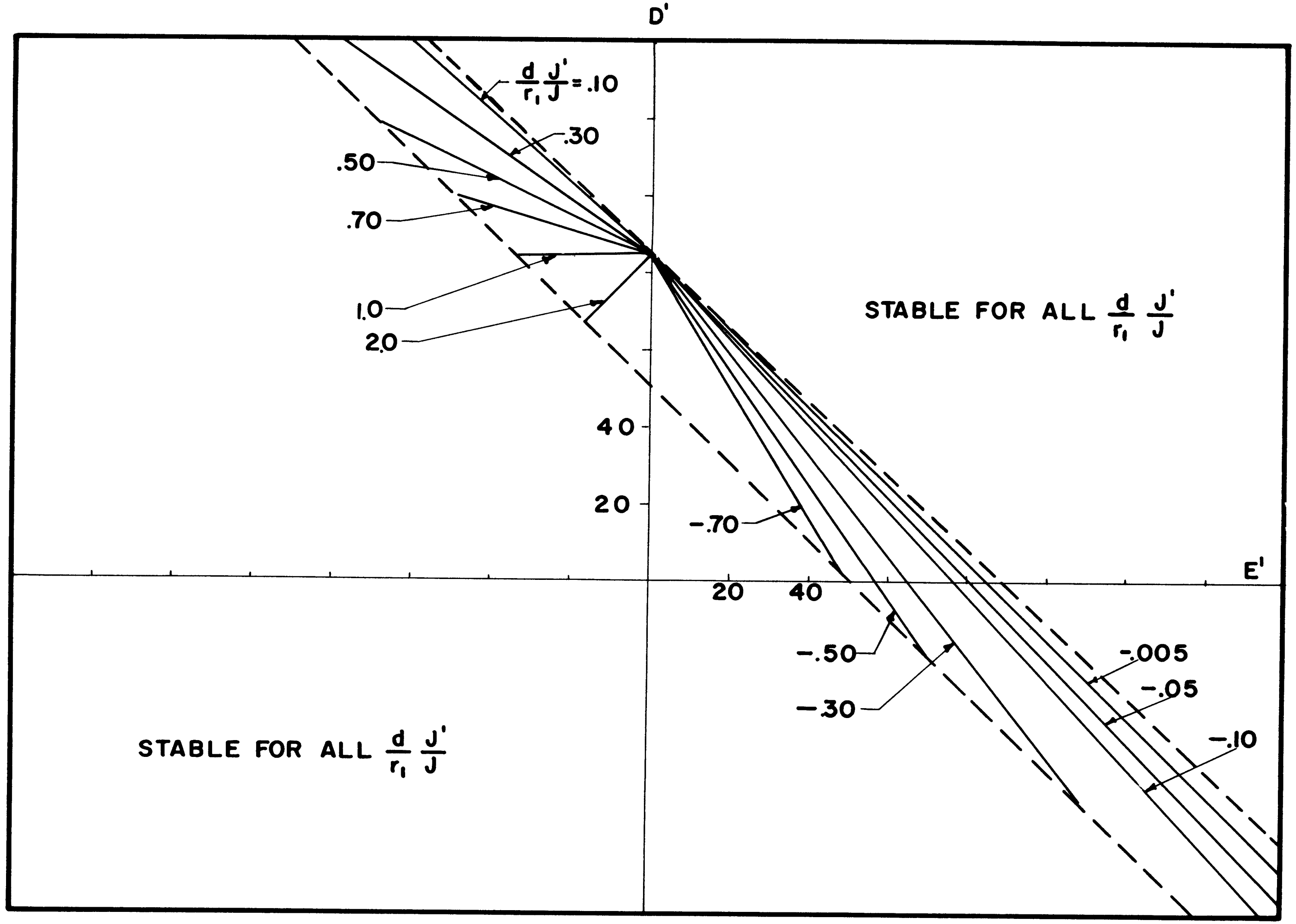

FIG. 4 MARGINAL STABILITY CURVES FOR C = 2500 AND

$\Omega_2 / \Omega_1 = 1.0$

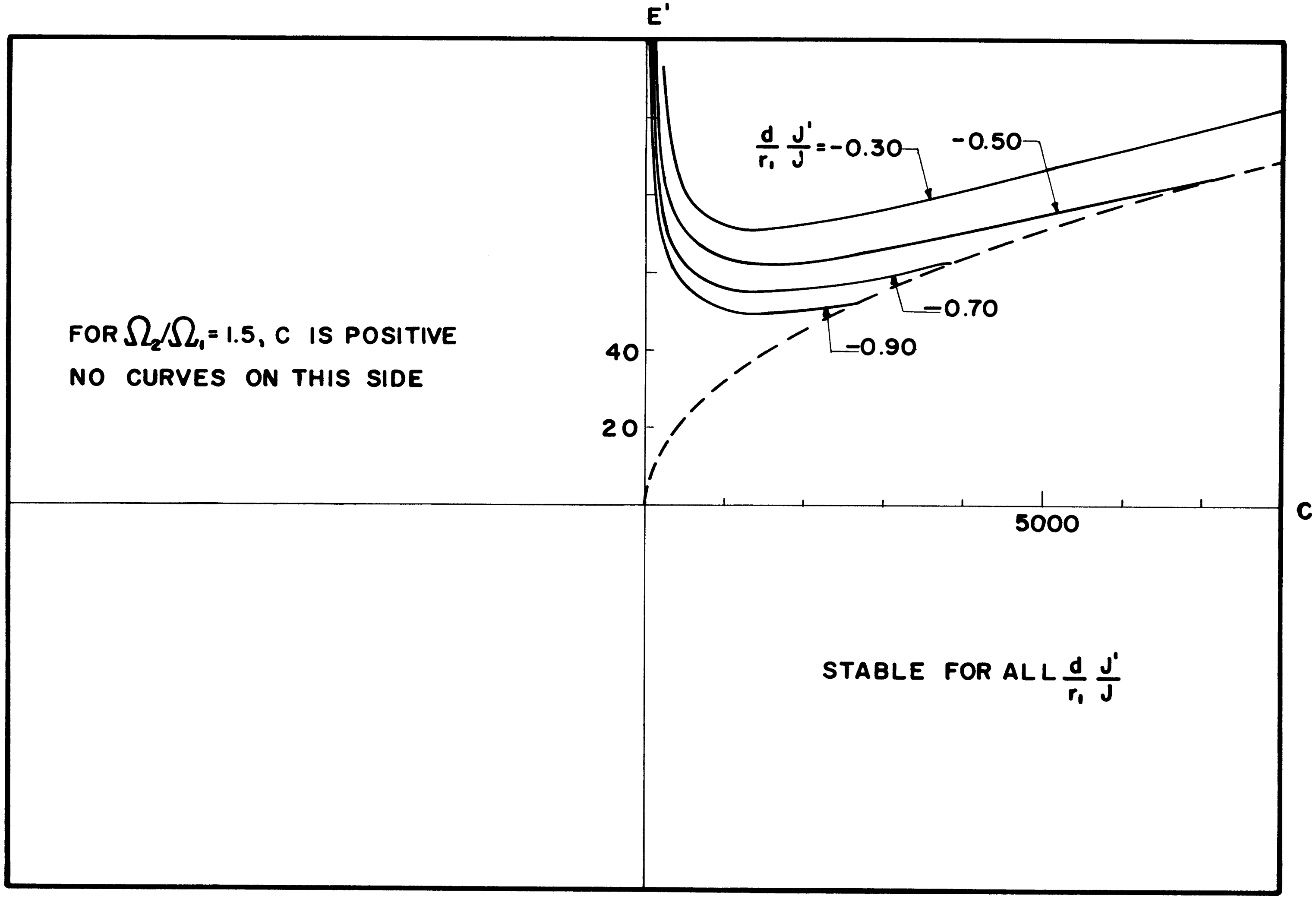

FIG.5 MAGINAL STABILITY CURVES FOR D' = 0 AND $\Omega_2/\Omega_1 = 1.5$

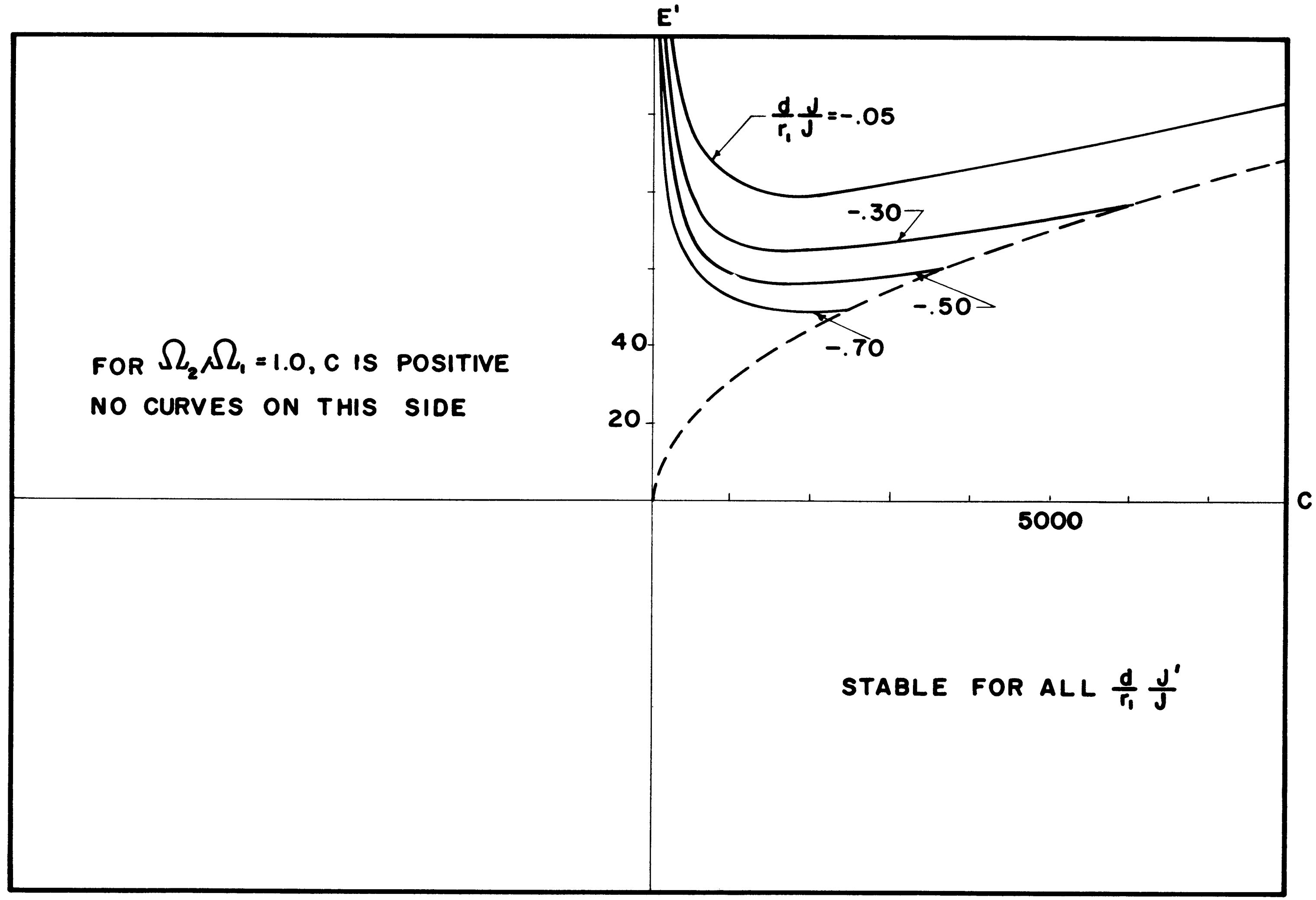

FIG. 6 MARGINAL STABILITY CURVES FOR D' = O AND

$\Omega_2/\Omega_1 = 1.0$

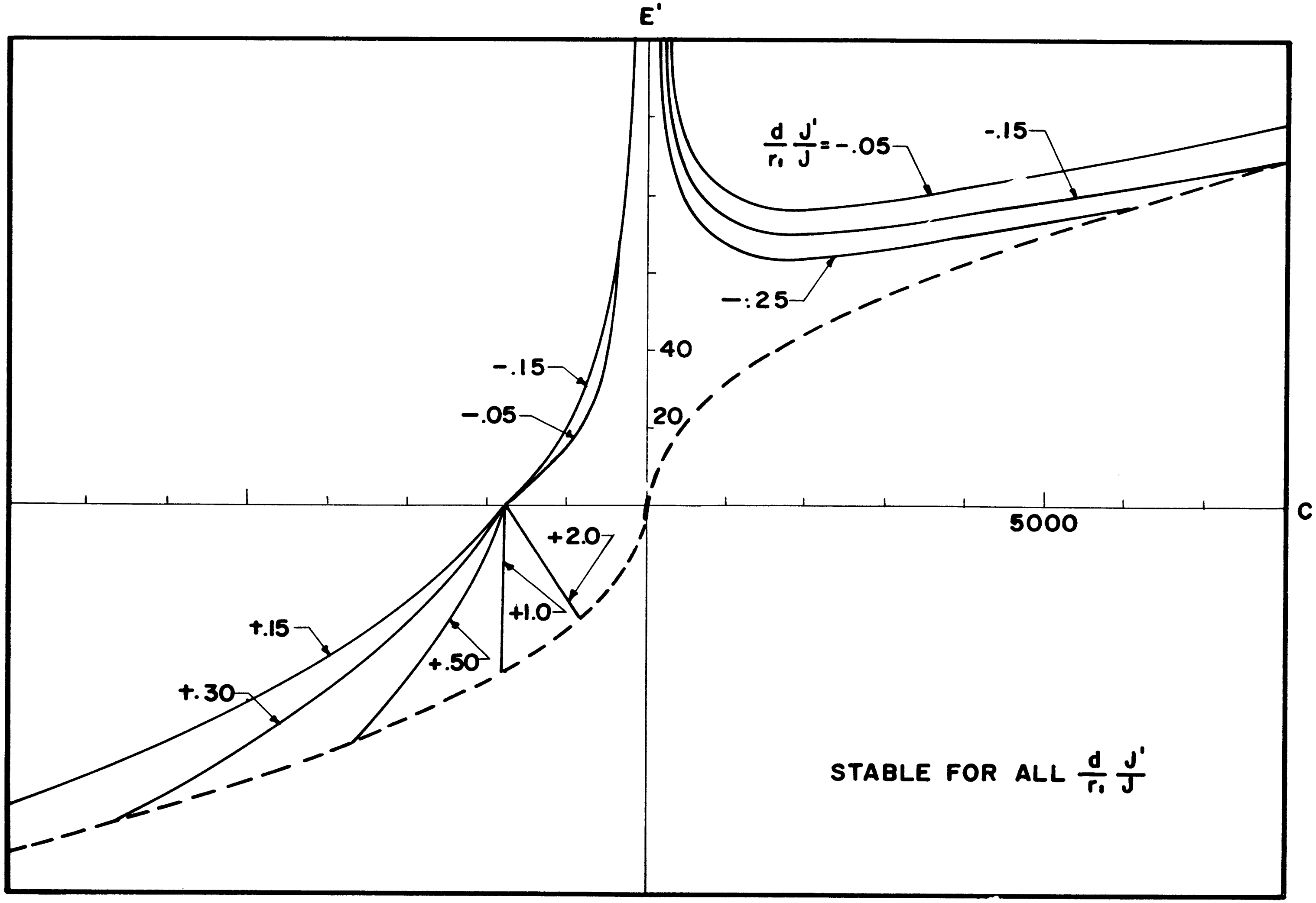

FIG 7 MARGINAL STABILITY CURVES FOR $D' = 0$ AND $\Omega_2/\Omega_1 = 0.9$

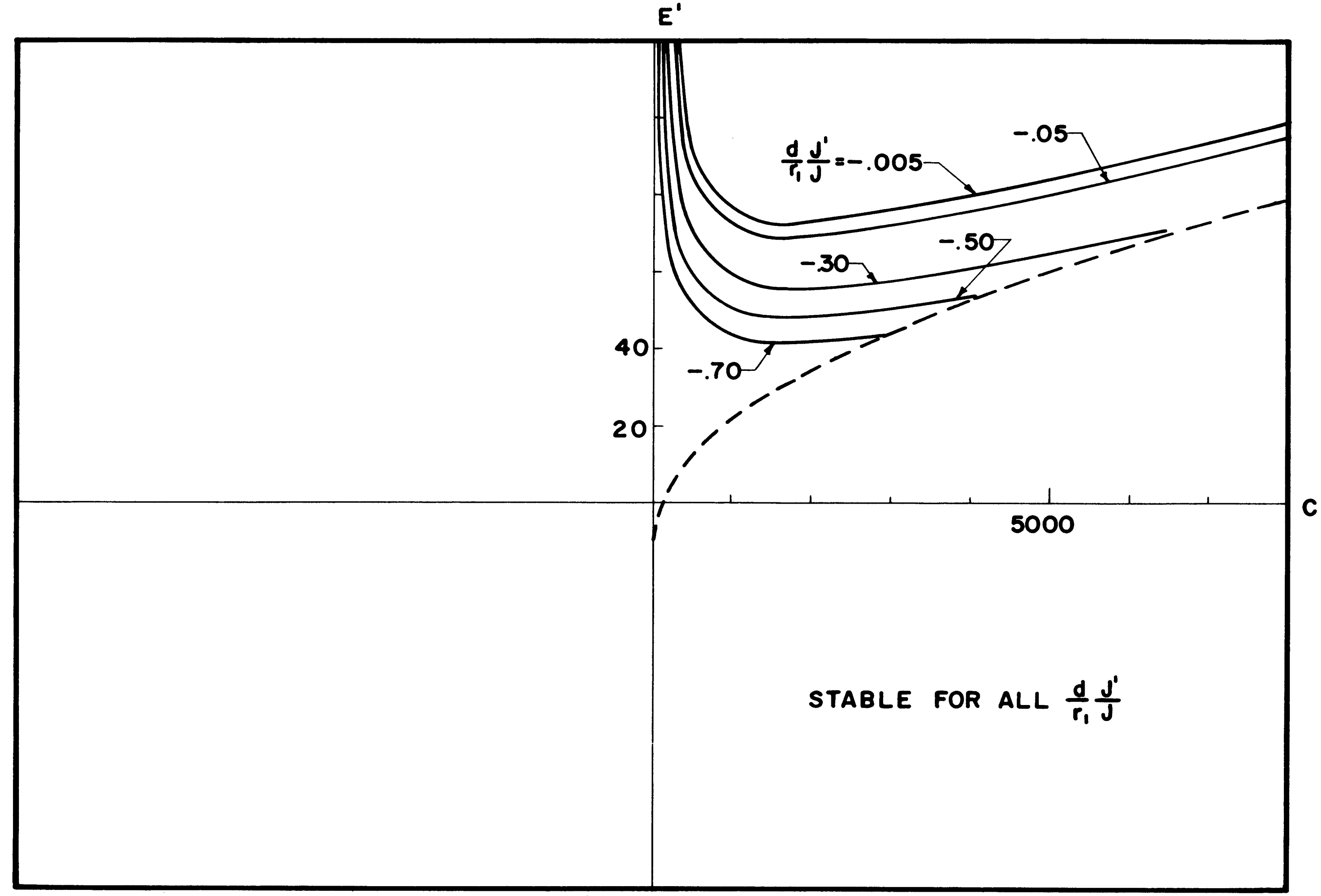

FIG. 8 MARGINAL STABILITY CURVES FOR D' = 10 AND $\Omega_2/\Omega_1 = 1.0$

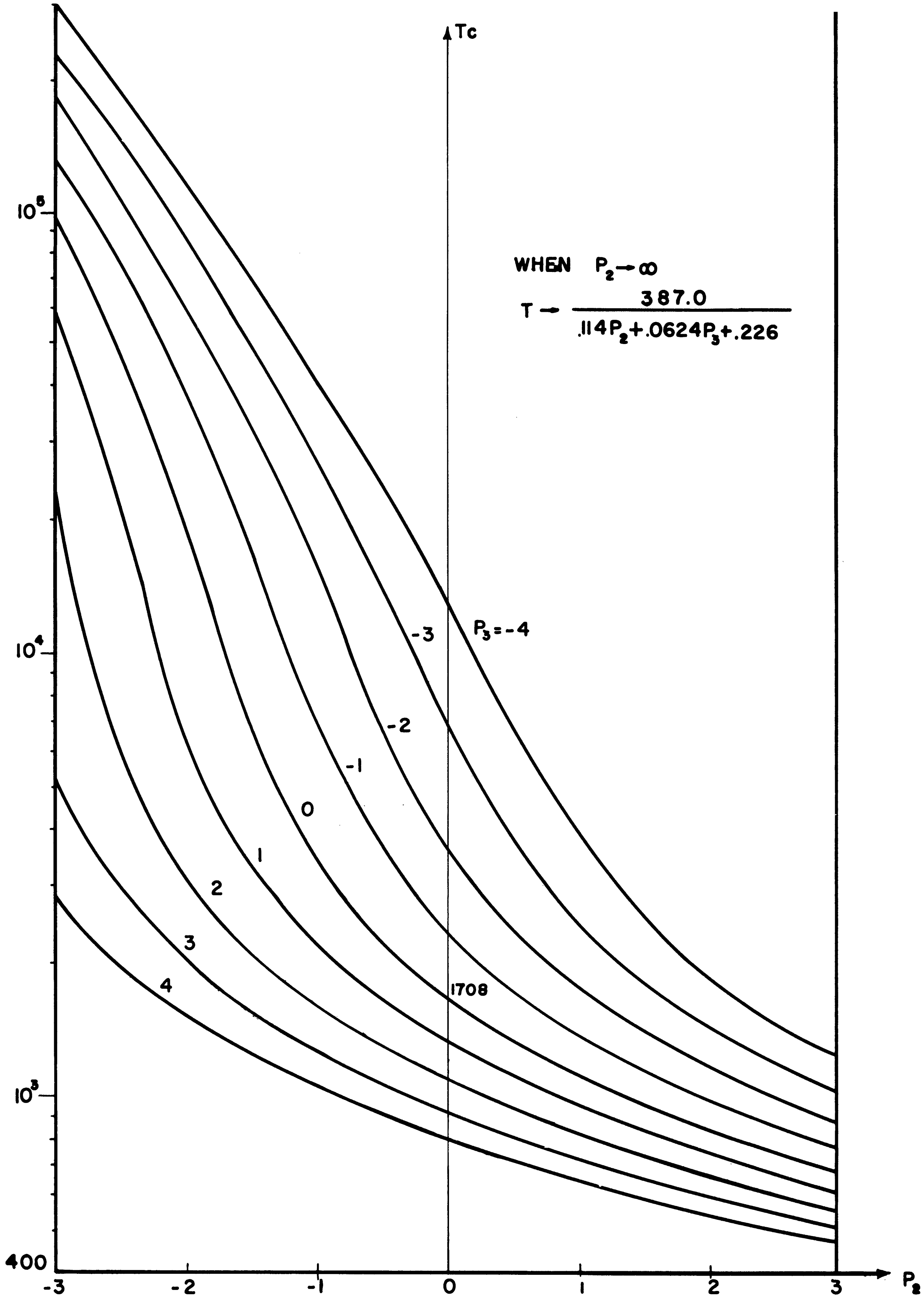

FIG. 9 CRITICAL TAYLOR NUMBER FROM EQUATION (66)

TABLE 1

CRITICAL TAYLOR NUMBER FOR P_3 = 4.0 AND VARIOUS ASSIGNED VALUES OF P_2 AND k

P_2	k	$T^{(n)}$ Obtained In The			
		First App.	Second App.	Third App.	Fourth App.
3.00	3.11	475.41	471.97	470.57	470.54
	3.12	475.41	471.95	470.56	470.53
	3.13	475.43	471.95	470.55	470.53
2.00	3.11	551.91	547.95	546.40	546.37
	3.12	551.90	547.93	546.39	546.35
	3.13	551.92	547.93	546.38	546.35
1.00	3.11	657.73	653.08	651.37	651.33
	3.12	657.73	653.06	651.35	651.31
	3.13	657.75	653.05	651.35	651.35
0.00	3.11	813.77	808.12	806.25	806.21
	3.12	813.77	808.10	806.22	806.18
	3.13	813.79	808.09	806.22	806.18
-0.5	3.11	923.29	916.97	915.03	914.98
	3.12	923.29	916.94	915.00	914.95
	3.13	923.29	916.94	915.00	914.95
-1.0	3.11	1066.9	1059.7	1057.7	1057.7
	3.12	1066.9	1059.7	1057.7	1057.7
	3.13	1066.9	1059.7	1057.7	1057.7
-1.5	3.11	1263.3	1255.1	1253.2	1253.1
	3.12	1263.3	1255.0	1253.2	1253.1
	3.13	1263.4	1255.0	1253.2	1253.1
-2.0	3.11	1548.5	1538.7	1537.3	1537.2
	3.12	1548.5	1538.7	1537.2	1537.1
	3.13	1548.5	1538.7	1537.2	1537.2
-2.5	3.11	1999.9	1988.0	1987.8	1987.7
	3.12	1999.9	1988.0	1987.7	1987.6
	3.13	2000.0	1988.0	1987.7	1987.7

TABLE 2

CRITICAL TAYLOR NUMBER FOR P_3 = 3.0 AND VARIOUS ASSIGNED VALUES OF P_2 AND k

P_2	k	$T^{(n)}$ Obtained In The			
		First App.	Second App.	Third App.	Fourth App.
3.00	3.11	514.94	511.72	510.09	510.07
	3.12	514.94	511.70	510.08	510.05
	3.13	514.95	511.70	510.08	510.05
2.00	3.11	605.89	602.25	600.41	600.39
	3.12	605.89	602.23	600.40	600.37
	3.13	605.91	602.23	600.40	600.37
1.00	3.11	735.87	731.69	729.59	729.56
	3.12	735.87	731.67	729.57	729.54
	3.13	735.89	731.67	729.58	729.54
0.00	3.11	936.87	931.99	929.58	929.55
	3.12	936.85	931.97	929.56	929.52
	3.13	936.88	931.97	929.56	929.53
-0.5	3.11	1085.1	1079.7	1077.2	1077.1
	3.12	1085.0	1079.7	1077.2	1077.1
	3.13	1085.1	1079.8	1077.2-	1077.1
-1.0	3.11	1288.9	1283.2	1280.5	1280.5
	3.12	1288.9	1283.2	1280.5	1280.5
	3.13	1288.9	1283.2	1280.5	1280.5
-1.5	3.11	1587.0	1581.1	1578.4	1578.4
	3.12	1587.0	1581.1	1578.4	1578.3
	3.13	1587.1	1581.1	1578.4	1578.4
-2.0	3.11	2064.7	2058.5	2056.7	2056.7
	3.12	2064.7	2058.5	2056.7	2056.6
	3.13	2064.7	2058.8	2056.7	2056.6
-2.5	3.11	2953.6	2949.3	2949.7	2949.7
	3.12	2953.6	2949.2	2949.7	2949.7
	3.13	2953.7	2949.3	2949.9	2949.8

TABLE 3

CRITICAL TAYLOR NUMBER FOR $P_3 = 2.0$ AND VARIOUS ASSIGNED VALUES OF P_2 AND k

P_2	k	$T^{(n)}$ Obtained In The First App.	Second App.	Third App.	Fourth App.
3.00	3.11	561.63	558.72	556.81	556.79
	3.12	561.63	558.71	556.80	556.77
	3.13	561.64	558.71	556.80	556.78
2.00	3.11	671.59	668.40	666.18	666.16
	3.12	671.58	668.39	666.17	666.14
	3.13	671.60	668.40	666.17	666.15
1.00	3.11	835.08	831.64	828.99	828.97
	3.12	835.08	831.63	828.97	828.95
	3.13	835.11	831.63	828.98	828.96
0.00	3.11	1103.8	1100.3	1097.0	1097.0
	3.12	1103.8	1100.2	1097.0	1097.0
	3.13	1103.8	1100.3	1097.0	1097.0
-0.5	3.11	1315.5	1312.1	1308.5	1308.4
	3.12	1315.5	1312.1	1308.4	1308.4
	3.13	1315.5	1312.1	1308.5	1308.4
-1.0	3.11	1627.5	1624.7	1620.7	1620.7
	3.12	1627.5	1624.7	1620.7	1620.6
	3.13	1627.6	1624.7	1620.7	1620.7
-1.5	3.11	2133.8	2132.2	2127.9	2127.9
	3.12	2133.7	2132.1	2127.8	2127.8
	3.13	2133.8	2132.2	2127.9	2127.9
-2.0	3.11	3097.2	3097.0	3093.6	3093.6
	3.12	3097.0	3097.0	3093.6	3093.6
	3.13	3097.1	3097.1	3093.6	3093.6
-2.5	3.10	5646.0	5614.2	5623.5	5623.3
	3.12	5645.6	5615.6	5623.0	5622.8
	3.14	5645.9	5615.6	5623.0	5622.8
-3.0	3.56	32571	21094	21305	21289
	3.58	32638	21094	21303	21287
	3.60	32708	21095	21304	21287

TABLE 4

CRITICAL TAYLOR NUMBER FOR $P_3 = 1.0$ AND VARIOUS ASSIGNED VALUES OF P_2 AND k

P_2	k	$T^{(n)}$ Obtained In The First App.	Second App.	Third App.	Fourth App.
3.00	3.11	617.63	615.15	612.87	612.85
	3.12	617.63	615.14	612.86	612.84
	3.13	617.65	615.15	612.87	612.84
2.00	3.11	753.26	750.73	747.98	747.96
	3.12	753.26	750.72	747.97	747.94
	3.13	753.28	750.73	747.97	747.95
1.00	3.11	965.22	962.84	959.39	959.37
	3.12	965.22	962.84	959.38	959.36
	3.13	965.24	962.86	959.39	959.37
0.00	3.11	1343.2	1341.6	1336.9	1336.9
	3.12	1343.2	1341.6	1336.9	1336.9
	3.13	1343.2	1341.6	1337.0	1337.0
-0.5	3.11	1670.2	1669.4	1663.9	1663.9
	3.12	1670.2	1669.4	1663.9	1663.9
	3.13	1670.2	1669.4	1663.9	1663.9
-1.0	3.11	2207.6	2207.6	2200.9	2200.9
	3.12	2207.6	2207.6	2200.9	2200.9
	3.13	2207.7	2207.7	2200.9	2200.9
-1.5	3.11	3255.2	3249.4	3241.4	3241.3
	3.12	3255.1	3249.3	3241.3	3241.2
	3.13	3255.2	3249.4	3241.4	3241.3
-2.0	3.14	6194.4	6041.7	6039.0	6037.8
	3.16	6195.6	6041.7	6038.9	6037.8
	3.18	6197.4	6042.2	6039.6	6038.4
-2.5	3.82	67345	20181	20335	20297
	3.84	67553	20180	20334	20296
	3.86	67768	20181	20334	20296
-3.0	5.24		74150	58359	58759
	5.26		74195	58357	58757
	5.28		74244	58358	58758

TABLE 5

CRITICAL TAYLOR NUMBER FOR P_3 = 0.0 AND VARIOUS ASSIGNED VALUES OF P_2 AND k

P_2	k	$T^{(n)}$ Obtained In The			
		First App.	Second App.	Third App.	Fourth App.
3.00	3.11	686.03	684.12	861.35	681.33
	3.12	686.03	684.12	681.33	681.32
	3.13	686.06	684.13	681.34	681.33
2.00	3.11	857.54	855.88	852.38	852.37
	3.12	857.54	855.88	852.37	852.36
	3.13	857.57	855.89	852.39	852.37
1.00	3.11	1143.4	1142.4	1137.7	1137.7
	3.12	1143.4	1142.4	1137.7	1137.7
	3.13	1143.4	1142.4	1137.7	1137.7
0.00	3.11	1715.1	1715.1	1707.9	1707.9
	3.12	1715.1	1715.1	1707.9	1707.9
	3.13	1715.1	1715.2	1708.0	1708.0
-0.5	3.11	2286.8	2284.8	2275.4	2275.4
	3.12	2286.8	2284.8	2275.4	2275.3
	3.13	2286.9	2284.9	2275.4	2275.4
-1.0	3.11	3430.2	3403.9	3390.6	3390.4
	3.12	3430.1	3403.8	3390.5	3390.3
	3.13	3430.3	3403.8	3390.5	3390.3
-1.5	3.15	6861.6	6433.5	6419.8	6416.8
	3.20	6867.7	6431.3	6417.8	6414.8
	3.25	6878.5	6433.5	6420.2	6417.1
-2.0	3.95		18618	18739	18681
	4.00		18615	18735	18677
	4.05		18621	18739	18681
-2.5	5.00		54045	46066	46256
	5.05		54095	46044	46237
	5.10		54160	46036	46232
-3.0	6.04			97078	95631
	6.05			97083	95624
	6.06			97089	95621

TABLE 6

CRITICAL TAYLOR NUMBER FOR P_3 = -1.0 AND VARIOUS ASSIGNED VALUES OF P_2 AND k

P_2	k	$T^{(n)}$ Obtained In The					
		First App.	Second App.	Third App.	Fourth App.	Fifth App.	Sixth App.
3.00	3.11	771.48	770.27	766.81	766.79		
	3.12	771.48	770.27	766.80	766.79		
	3.13	771.51	770.29	766.82	766.81		
2.00	3.11	995.34	994.69	990.07	990.06		
	3.12	995.35	994.70	990.07	990.06		
	3.13	995.38	994.73	990.09	990.08		
1.00	3.11	1402.2	1402.2	1395.4	1395.4		
	3.12	1402.2	1402.2	1395.4	1395.4		
	3.13	1402.3	1402.2	1395.4	1395.4		
0.00	3.11	2371.8	2363.1	2350.7	2350.6		
	3.12	2371.8	2363.1	2350.7	2350.6		
	3.13	2371.9	2363.1	2350.7	2350.6		
-1.0	3.24	7706.2	6748.5	6725.9	6719.6		
	3.26	7712.4	6747.7	6725.2	6718.9		
	3.28	7719.4	6747.7	6725.3	6718.9		
-1.5	4.08		17049	17148	17075		
	4.10		17050	17148	17975		
	4.12		17052	17149	17076		
-2.0	4.96		42182	37611	37649		
	4.98		42200	37609	37648		
	5.00		42220	37608	37649		
-2.5	5.84		263412	744131	744745		
	5.86		263381	744211	744741		
	5.88		263349	744318	744768		
-3.0	6.70			154486	135140	135805	135614
	6.75			154624	135127	135792	135604
	6.80			154787	135132	135797	135611

TABLE 7

CRITICAL TAYLOR NUMBER FOR P_3 = -2.0 AND VARIOUS ASSIGNED VALUES OF P_2 AND k

P_2	k	$T^{(n)}$ Obtained In The First App.	Second App.	Third App.	Fourth App.	Fifth App.	Sixth App.
	3.11	881.24	880.79	876.34	876.34		
3.00	3.12	881.24	880.80	876.34	876.34		
	3.13	881.28	880.82	876.36	876.36		
	3.11	1185.9	1185.9	1179.5	1179.5		
2.00	3.12	1185.9	1185.9	1179.5	1179.5		
	3.13	1186.0	1186.0	1179.6	1179.6		
	3.11	1812.6	1808.7	1797.9	1797.8		
1.00	3.12	1812.6	1808.7	1797.9	1797.8		
	3.13	1812.7	1808.7	1797.9	1797.9		
	3.15	3844.5	3704.4	3679.9	3678.5		
0.00	3.16	3845.1	3704.4	3679.6	3678.5		
	3.17	3846.4	3704.6	3679.8	3678.7		
	3.30	8789.3	6966.8	6938.4	6927.8		
-0.5	3.35	8816.4	6963.7	6935.9	6925.1		
	3.40	8849.2	6964.6	6937.4	6926.4		
	4.10		15642	15727	15642		
-1.0	4.15		15640	15724	15640		
	4.20		15645	15728	15644		
	4.85		34359	31589	31528		
-1.5	4.90		34388	31583	31524		
	4.95		34427	31585	31530		
	5.60		126901	59141	59500		
-2.0	5.65		127078	59143	59496		
	5.70		127284	59158	59504		
	6.40			112478	105729	105964	105762
-2.5	6.45			112548	105711	105952	105750
	6.50			112639	105712	105958	105758
	7.25			277656	178892	178988	178930
-3.0	7.30			277896	178895	178956	178904
	7.35			278219	178929	178955	178912

TABLE 8

CRITICAL TAYLOR NUMBER FOR P_3 = -3.0 AND VARIOUS ASSIGNED VALUES OF P_2 AND k

P_2	k	T(n) Obtained In The First App.	Second App.	Third App.	Fourth App.	Fifth App.	Sixth App.
	3.11	1027.4	1027.4	1021.5	1021.5		
3.00	3.12	1027.4	1027.4	1021.5	1021.5		
	3.13	1027.4	1027.4	1021.5	1021.5		
	3.11	1466.7	1464.7	1455.3	1455.3		
2.00	3.12	1466.7	1464.7	1455.3	1455.3		
	3.13	1466.8	1464.7	1455.3	1455.3		
	3.12	2562.5	2519.7	2500.8	2500.4		
1.00	3.13	2562.6	2519.7	2500.7	2500.3		
	3.14	2562.8	2519.7	2500.7	2500.3		
	3.40	10262	7075.3	7045.8	7029.8		
0.00	3.45	10308	7072.4	7043.6	7027.5		
	3.50	10360	7073.4	7045.3	7029.0		
	4.15		14407	11482	14390		
-0.5	4.20		14407	11481	14389		
	4.25		14413	14485	14394		
	4.80		28910	27113	26995		
-1.0	4.85		28933	27109	26995		
	4.90		28965	27114	27002		
	5.45		81505	48372	48662		
-1.5	5.50		81647	48372	48662		
	5.55		81809	48383	48673		
	6.15			86451	84403	84323	84161
-2.0	6.20			86484	84387	84313	84150
	6.25			86533	84385	84317	84155
	6.95			178214	139994	140705	140426
-2.5	7.00			178407	139993	140696	140421
	7.05			178626	140008	140704	140433
	7.60			852572	230959	225239	225709
-3.0	7.65			850277	230973	225129	225607
	7.70			848723	230987	225041	225529

BIBLIOGRAPHY

PART ONE

Bieberbach, L. Conformal Mapping. New York: Chelsea Publishing Co.

Milne-Thomson, L. M. Theoretical Hydrodynamics. New York: The Macmillan Co.

Streeter, V. L. Fluid Dynamics. New York: McGraw-Hill Book Co.

PART TWO

Churchill, R. V. Fourier Series and Boundary Value Problems. New York: McGraw-Hill Co.

Fraenkel, L. E. "On the Flow of Rotating Fluid Past Bodies in a Pipe." Proc. Roy. Soc. A, 253, (1956) 506-26.

Lamb, H. Hydrodynamics. New York: (1932) Dover Publications, Inc.

Lamb, H. "On the Effect of the Walls of an Experimental Tank on the Resistance of a Model." Rep. Memor. Aero. Res. Comm., Lond., (1926) No. 1010.

Long, R. R. "Steady Motion Around a Symmetrical Obstacle Moving Along the Axis of a Rotating Liquid." J. Met. 10, (1953) 197-203.

Long, R. R. "Sources and Sinks at the Axis of a Rotating Liquid." Quart. J. Mech. and Appl. Mech., 9 (1956) 385-93.

Rayleigh, J. W. S. "The Form of Standing Waves on the Surface of Running Water." Proc. Lond. Math. Soc., 15, (1883) 69-82.

Squire, H. B. "Rotating Fluids." Surveys in Mechanics, (1955) Cambridge University Press.

Stewartson, K. "On the Slow Motion of a Sphere Along the Axis of a Rotating Liquid." Proc. Cambr. Phil. Soc., 48, (1952) 168-177.

Taylor, G. I. "The Motion of a Sphere in a Rotating Liquid." Proc. Roy. Soc. London, A, 102 (1922) 180-89.

Yih, C. S. "Exact Solutions for Steady Two-dimensional Flow of a Stratified Fluid." J. Fluid Mech., 9, Part 2, (1960) 161-74.

PART THREE

Chandrasekhar, S. "The Stability of Viscous Flow Between Rotating Cylinders in the Presence of a Radial Temperature Gradient." J. Rat. Mech. and Analy., 3, (1954a) 181-207.

Chandrasekhar, S. "The Stability of Viscous Flow Between Rotating Cylinders." Mathematika, 1, (1954b) 5-13.

Cowling, T. G. Magnetohydrodynamics. Interscience Tracts on Physics and Astronomy.

Lin, C. C. The Theory of Hydrodynamic Stability. (1955) Cambridge University Press.

Pellew, A. and Southwell, R. V. "On Maintained Convective Motion in a Fluid Heated from Below." Proc. Roy. Soc., A, 176, (1940) 312-343.

Stommel, H. et al. "An Oceanographical Curiosity: The Perpetual Salt Fountain." Deep-Sea Research, 3, (1956) 152-153.

Synge, J. L. "On the Stability of a Viscous Liquid Between Two Rotating Coaxial Cylinders." Proc. Roy. Soc. A, 167, (1938) 250-256.

Taylor, G. I. "Stability of a Viscous Liquid Contained Between Two Rotating Cylinders." Phil. Trans. A, 223, (1923) 289-343.

Yih, C. S. "Ring Vortices Generated Electromagnetically." J. Fluid Mech., 5, (1959a) 436-44.

Yih, C. S. "Inhibition of Hydrodynamic Instability by an Electric Current." The Physics of Fluids, 2, (1959b) 125-130.

Yih, C. S. "The Dual Role of Viscosity in the Instability of Revolving Fluids of Variable Density." The Physics of Fluids, Aug. 1961.